Study Of Pressure Driven Flow Of Laponite Suspension Through A Cylindrical Tube

by

Prophesar M. Kamdi
AcSIR Registration Number: 20EE14A26053

A thesis submitted to the
Academy of Scientific & Innovative Research
for the award of the degree of
DOCTOR OF PHILOSOPHY
in
ENGINEERING

Under the supervision of
Dr. Ashish V. Orpe,
Dr. Guruswamy Kumaraswamy

CSIR- National Chemical Laboratory, Pune

Academy of Scientific and Innovative Research
AcSIR Headquarters, CSIR-HRDC campus
Sector 19, Kamla Nehru Nagar,
Ghaziabad, U.P. – 201 002, India

December 2021

Certificate

This is to certify that the work incorporated in this Ph.D. thesis entitled, "*Study of pressure driven flow of Laponite suspension through a cylindrical tube*", submitted by *Prophesar M. Kamdi* to the Academy of Scientific and Innovative Research (AcSIR) in fulfillment of the requirements for the award of the Degree of *Doctor of Philosophy in Engineering*, embodies original research work carried-out by the student. We, further certify that this work has not been submitted to any other University or Institution in part or full for the award of any degree or diploma. Research material obtained from other source and used in this research work has/have been duly acknowledged in the thesis. Images, illustration, figures, table, etc., used in the thesis from other sources, have also been duly cited and acknowledged.

(Student)	(Co-supervisor)	(Supervisor)
Propphesar M. Kamdi	Dr. Guruswamy Kumaraswamy	Dr. Ashish V. Orpe
20/12/2021	20/12/2021	20/12/2021

STATEMENTS OF ACADEMIC INTEGRITY

I, Prophesar Madhukar Kamdi, a Ph.D. student of the Academy of Scientific and Innovative Research (AcSIR) with Registration No. 20EE14A26053 hereby undertake that, the thesis entitled "Study of pressure driven flow of Laponite suspension through a cylindrical tube" has been prepared by me and that the document reports original work carried out by me and is free of any plagiarism in compliance with the UGC Regulations on *"Promotion of Academic Integrity and Prevention of Plagiarism in Higher Educational Institutions (2018)"* and the CSIR Guidelines for "*Ethics in Research and in Governance (2020)".*

Student

Date : 20/12/2021
Place : NCL - Pune

It is hereby certified that the work done by the student, under my/our supervision, is plagiarism-free in accordance with the UGC Regulations on *"Promotion of Academic Integrity and Prevention of Plagiarism in Higher Educational Institutions (2018)"* and the CSIR Guidelines for "*Ethics in Research and in Governance (2020)".*

Co-supervisor

Name : Dr. Guruswamy Kumaraswamy
Date : 20/12/2021
Place : IIT - Bombay

Supervisor

Name : Dr. Ashish Orpe
Date : 20/12/2021
Place : NCL - Pune

Dedicated to my three Aunts, my maternal Grandmother and my family.....

Acknowledgements

Well, it is totally unbelievable moment to me that I have wound up my research work over here. The last 3 years look like 3 decades and it feels like spent major period of my life. But finally I made it, thanks to those who helped me professionally/ non-professionally along the way, without them I would have "Mr. Nobody" and might have lost the track completely. It is my greatest honor that I could contribute to science and technology through this research work.

Hereby I would like to express my sincere thanks to my supervisors: Dr. Ashish Orpe for introduction of such interesting, quite challenging and fundamental research problem, for help in data analysis, for experimental help, for scientific writing, for programming, and for other professional and non-professional guidance; and Dr. Guruswamy Kumaraswamy for encouraging discussion, backing, advices in every aspects, asking rigorous questions, financial help and other supports. They go very down to any problem so that nothing miss out. I am sure they can even do medical surgery even though it is not their area, if situation comes. It is worth to acknowledge that excellent understanding about the topic, high standards of integrity and humanity are few eminent qualities found in my advisors. I find myself lucky to have such wonderful advisors and thanks for bearing me during this period.

A very sincere note of thanks to my doctoral advisory committee members, Dr. Sarika Bhattacharyya, Dr. Chetan Gadgil, Dr. Narshinha Argade and Dr. Ashish Lele for their constant support, encouragement and suggestions throughout my Ph. D. and for being always soft-hearted. Also I am extremely thankful to Dr. Amol Kulkarni, who helped me by providing access to his lab and allowed me to use his instrumental facility at the beginning of thesis work, without asking any questions.

This section belongs to those who have taken significant efforts and excellent contributions to have their acknowledgement over here. Thank you Muzammil Khan for using me as your debit card, thank you Akash Sharma for wasting my time on nonsense chat, thank you Aniket Joshi for being as own and thank you Mrityunjay Sharma for being occasional visitor. Apart from this which you may not like it, I like you all. Here, I would like to refer one south Indian movie (Sarrainodu) scene of 'Allu Arjun and Brahmanandam', where Brahmanandam says that he cannot lie. Like him

I cannot “lie” my friends. I am grateful that I have such trustful ‘besties’ and also grateful for your all helps, without you it would be an unpleasant life at NCL, Pune.

I think for every researcher working place is the primary home and so to me is room no. J-104 (Dr. Guruswamy’s lab) of PAML building. It is a miniature of real world where I have watched changing sky shades every moment, many good mornings, to and fro moving people, visitors, etc. as well as extreme silence in the corridor of J-wing, chirping birds and may more activities through wide windows on either sides of my experimental setup. The lab has very special value in my life and here I would like to thank my labmets from this lab. Thanks Bipul Biswas for utilizing my very precious experiment running time to a side by side discussion, making experimental lab musical, organizing weekdays plan and other things. He is the special person with whom I spend most of the time other that my experimental time. Probably he is the best person who knows me very well apart from my classmate besties, labmets and other close friends. Well this platform I would like to take an opportunity to thank Dr. Karthika, my labmet, friend and even more valuable than any. I feel energetic whenever you work around. Thanks Dr. Manoj Sharma and Dr. Soumyajyoti Chatterjee for being fair weather friends. I have learn a lot from you and also thankful for being generous and friendly all the time. I must give credits to Dr. Manoj Sharma for shifting my experimental setup over here in J-104. Thanks Saurabh Usgaonkar, Aniket Gudadhe and Subrajeet Deshmukh for taking us to a relaxing Sunday feast, for making movie plans and for all fussy gossips. Also thanks for introducing ‘Zarana’ term that was one time computer password for few days. Miss Suranjana, thanks for the lift although it was car’s effort. You can assume this comment irrelevant because I usually don’t thank my close friends and best of luck for your future ahead. I am extremely grateful that I have crossed paths of Dr. Anees and Dr. Nirmalya.

Now I would like to thank my labmets cum friends from Dr. Ashish Orpe’s lab. Dr. Sameer Huprikar and Mr. Mayuresh Kulkarni presence I feel as my elder brothers. Thank you for guiding me all time, for a help in visualization setup, for software help, for deeper discussion, for mini tea parties, etc. There is another sensational, super-cool lady, Dr. Subhadarshinee Sahoo, I would like to express my sincere thank for MATLAB help, for sharing her opinions and for the advices although I have not listen to that and it did not work in my case. Thank you Dr. Bhavna Vyas madam, Ms. Sukhada, Ms. Divika and Mr. Ravindra for giving me lovable company and for

everything that we did at NCL. My association with all these peoples has made my stay pleasant and memorable. At last, I owe an apology to you all if you are hurt by me by any means. It was never ever my intention.

Whatever I achieved or did not succeed, one thing was always same and never ever changed that is my family. It is my deepest gratitude to my three aunts (Mandabai, Sugandhabai and Mangalabai) and my grandmother (Muktabai) for believing in me, for loving especially me, for being constantly by my side and for every other thing that I am not aware of till now. Also, I like to thank Rushi kakaji, my brothers (Roshan, Mithun, Sagar and very young lady 'Swaralee') and my parents for giving me such wonderful family. Apart from this there is one enemy consistent all the time, to whom I don't like to thank and want to be away from as that person has provided plenty reasons to hate. But I hearty thankful to that person for keeping two-wheeler seat reserved for me every time, for making surprise plans of tracking, for giving nonsense reasons and excuses to celebrate each day (I really don't know why do you do this?), for being an excellent cook (that unlikely imposed the burden on me cleaning all those utensils), for not being so surprised what other have done, for being my 'antivirus' to keep the all junk away and for being my 'Besty' all the time. Thank you Amit Chaudhary. This is an extremely small word to expresses my gratitude. I know you won't care this but still. So that you could offer me a 'Gaming system' as a gift, if you read/ know this by chance. Thank you….

Kamdi Prophesar

December – 2021

Contents

List Of Figures

List Of Tables

Chapter - 1

1 Introduction

1.1 Introduction to flow clogging

Any flowing material can be subject to clogging. The term ‘flow’ refers to motion while "clogging" phenomena restricts the motion. Various industrial applications handle materials as two phase systems, viz., suspensions, gels, emulsions, foams, crude oil. All these materials comprise constituents or entities suspended in continuous medium. Such materials while flowing through conduits, orifices, channels etc. have a tendency to block the flow. The blockage results in reduced cross sectional area available for flow. This can occur when the size of the individual constituent or entities are of the same order as the length scale of the available flow region (e.g. jamming of suspension when the size of an orifice is of the order of a few particle diameters in the suspension). In another scenario, the constituents may be small compared to flow area but they may agglomerate over time leading to bigger entities which block the flow (e.g. flow of crude oil through pipelines). A time dependent or a thixotropic fluid can cause such type of clogging. In everyday life as well we see above types of blocking during flow of water through kitchen sink, bathroom or during flow of blood through arteries and veins. Investigating the phenomena of flow and clogging caused due to time varying state of the material flowing through pipes forms the primary objective of this work.

1.2 Flow through pipes/capillaries

Flow regime of liquids through pipes can range from creeping flows to turbulent flows [1, 2]. The occurrence of these flows is governed by the well-known dimensionless number, Reynolds number relating the inertial components to the viscous components. The creeping and laminar flows are associated with steady parallel streamlines oriented along flow direction while turbulent flow is characterized by several disturbances, instabilities, and vortices which ensure the non-existence of flow streamlines. The former is associated with minimal fluid mixing while the latter leads to significant mixing. For laminar flow through a pipe, the pressure drop encountered during the flow is given by the famous Hagen-Poiseuille equation as [3]

$$\frac{\Delta P}{L} = \frac{128\,\mu\,Q}{\pi\,D^4} \tag{1.1}$$

where, P is the pressure, L is the pipe length, μ is the fluid viscosity, Q is the flow rate and D is the pipe dimension. For a fixed fluid and pipe dimensions, the pressure drop is directly proportional to the flow rate. Further, a higher pressure is needed to pump the fluid of higher viscosity at the same flow rate and vice-versa through a pipe of same dimensions. Variants of eq. 1.1. can be obtained for different types of fluids, viz. shear thinning or thickening fluids or yield stress fluids [3, 4]. In each case, the primary variable influencing the pressure drop is the viscosity term whose dependence on shear rate is as expressed in the stress constitutive equation [2, 5]. For suspensions, an additional dependence on particle fraction needs to be accounted for expressing the viscosity in addition to the shear rate dependence [6-8]. In all the cases, however, the pressure drop always varies directly with the applied flow rate. In certain cases, the surfaces (either chemically modified or as it is) can exhibit different affinity with the flowing liquid, thereby causing it to slip [9, 10]. In such cases, a lesser pressure is required for the same flow rate compared to that with no slip conditions.

The situation is, however, quite complicated for a material with time dependent properties (e.g. clay suspensions). Such materials “age” with time. The aging corresponds to temporal evolution of the material microstructure and rheology during storage. For such cases, it is not possible to define the stress constitutive equation unambiguously. The viscosity in such cases depends on time in addition to shear rate and possibly particle fraction. Consequently, a relatively simpler variant of eq. 1.1 is not possible to derive, thereby posing problems in ascertaining the

flow rate-pressure drop relations during flow of such materials. Not surprisingly, the studies on the flow of such materials through pipes remain quite inadequate. However, many such time dependent materials handled in industrial systems as well as in biological systems do flow through pipes or capillaries, rigid or flexible, under constant or variable pressure, at constant or varying temperature. Understanding the flow behavior of such time dependent materials through capillary/pipe is quite necessary from the perspective of their design, handling and their propensity to clog the flow over time. In the following, we describe two such systems which form the motivation for the thesis work.

1.3 Flow of ageing fluids through pipes

We present two examples from diverse areas which constitute the flow of a time dependent material through pipe-like system. Both systems show similar behavior in terms of the accumulation of material along the pipe wall with time leading to flow clogging. In both cases, such clogging can cause irreversible damage, may require substantial efforts in removing the clogged sections and in some instances replacing the pipe section itself. It is curious to note that such diverse systems can exhibit similar behavior thereby implying common analysis and solution which may be applied to both systems and is derived from studying of a simple model system.

The blood vessels in the human body are conduits with approximately circular cross-section, that carry blood under pressure. A wide range of blood vessels are found in the human body. Artery (with diameter D = 35µm -25mm, and wall thickness = 30µm – 2mm) and vein (with diameter D = 20µm -30mm, and wall thickness = 3µm – 1.5mm) are the blood vessels that transport blood from the heart and to the heart respectively [11, 12]. Typically, blood vessels are subjected to pulsating pressurized blood flow at pressures as high as 90 mmHg. Blood flow can be interrupted by cell growth, waste deposition, plaque formation and scar tissue deposition. These obstructions are evident and can impair organ functioning by obstructing blood flow [13, 14]. At present, cardiovascular diseases (CVDs) are the major complications in health care. In 2016 report by WHO, near about 31% of global deaths are from CVDs [15]. 17 million deaths are estimated to happen every year caused by attack and stroke.

The constituents like fat, cholesterol etc. present in the blood can accumulate on blood vessel wall which harden over period of time to form deposits known as plaque. Plaque grows

further and eventually blocks the blood vessels. This can also happen suddenly leading to a stroke [16, 17] (see fig. 1.1). In other cases, narrowing blood vessel is subjected to pressurized blood flow. As a result, blood vessel becomes weaker and develops balloon-like shape which can burst easily [18, 19]. Vessel rupture cause brain tissue death because of bleeding, which results in permanent or temporary paralysis of patient and even patient death. In medical practices, endoscopy is used to place a stent into blocked passages in the body. But over time the inserted stent also suffers from blockages [14, 20-22]. Thus, stent replacement is needed incurring additional health care cost and worsening the patient's quality of life.

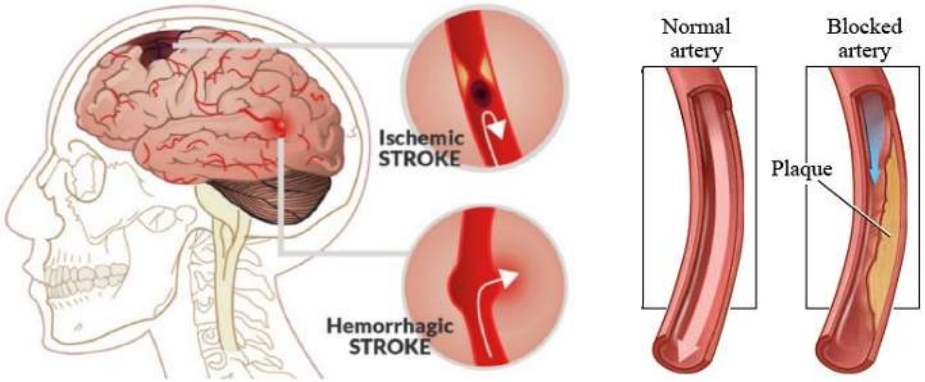

Figure 1.1 Schematic of narrowing, blocked and ruptured blood vessel as a consequence of growing plaque inside a normal vessel. This figure has been reprinted with permission from TND and UCSF [23, 24].

Figure 1.2 Blocked petroleum pipeline during stutdown period. This figure is reprinted from [25].

In a similar vein, blockage in pipeline is a severe issue encountered in the crude oil industry necessitating restart. During normal operation, wax deposition on the pipe wall leads to pumping load exceeding the pump limit that operates at constant pressure. Therefore, throughput decreases which further enhances wax deposition. In order to maintain constant operating pressure and flow rate, periodic or emergency shutdowns are implemented. Once a plant shuts down, crude oil becomes thicker, forming gel like waxy material in the long pipeline (see fig. 1.2). Such a blocked pipeline cannot restarted by normal operation. Sometimes, it needs a pressure higher than designed one to restart flow. In that case, whole pipeline needs to be cleaned manually. Apart from shutdown procedure, there is a pigging operation that removes wax deposits from pipe wall during normal operation [26, 27]. A “pig” is inserted into the pipeline via a pig launcher. This pig removes the deposits in the pipeline until it reaches the pig receiving station. This operation is called pigging. So, continuous monitoring and frequent pigging of pipelines can prevent the plant shutdown frequency to some extent. But, the operation effectiveness is limited to certain deposit thickness and certain deposit quality.

1.4 Scope of this thesis

This study focuses on pressure driven fluid flow through a pipe in a scenario where complete flow blocking may occur. Time dependent flow characteristics and mechanism of flow blocking are the

primary expected outcomes of this study which would set the stage for designing of flow assemblies to avoid blocking, and to develop mathematical models for prediction of overall flow behavior. In this regard, a suitable material which has time dependent characteristics is chosen as a model system. The overall methodology involves designing of the flow system while accounting for all possible issues arising out of the time dependent nature of the material. Flow rate and pressure variations are the primary measurements accompanied by flow visualization for qualitative understanding.

1.5 General objectives

The general objectives of this work are listed below:

1. To design an experimental system and methodology for the pipe flow study of time dependent material.
2. To study in-situ flow blocking behavior and transient behavior of time dependent suspension during pressure driven flow through a tube.
3. To experimentally investigate the influence of parameters such as pipe diameter, pipe length, time scale associated with material properties, flow rate, etc. during flow of material through a pipe.

1.6 Thesis outline/ structure

First chapter provides general introduction to the flow of fluids through pipes with focus on suspensions and is accompanied with description of relevant applications. The chapter also defines the scope and general objectives.

A detailed review of relevant published work is provided in chapter 2 focusing on various aspects related to flow of suspensions, such as rheology, flow profiles, clogging, restart etc. Towards the end, the gaps in the literature are identified followed by clearly stated objectives.

The details of experimental system, primarily its evolution, along with some novel designs are discussed in chapter 3. The final system is designed to counter the difficulties arising out of time dependent model fluid considered.

Chapter 4 is focused on studying the slip behavior during the flow of Laponite suspensions through pipes. The main feature of this chapter is the non-intuitive pressure-flow rate behavior and the reasonable scaling achieved accounting for various flow variables,

The concluding remarks and suggestions for possible directions to be followed in future are described in chapter 5.

Chapter - 2

2 Literature Review

Suspensions, i.e. particles suspended in a liquid, are often transported through pipes in many industrial operations. Flow of suspensions, under different circumstances, encounter resistance thereby slowing the flow or complete blocking. Flow clogging can be expected to occur due to time or shear dependent agglomeration of individual particles in a suspension when subjected to different operating conditions like temperature, flow rate, pipe material, particle concentration, pipe diameter. Such clogging problems can block the pipelines permanently thereby requiring immense efforts in flow start-up. Understanding this flow clogging behavior requires detailed knowledge about rheology and microstructure of the suspension. In the following sections, we will discuss the relevant literature related to above mentioned various facets of pipe flow of suspensions. Towards the end we will outline some of the problems identified for further research.

2.1 Pressure driven flow in pipes

Substantial body of work exists in literature focused on studying various aspects of flow suspensions through pipes and channels. In the following, we primarily focus on the studies related to pressure driven flow of time dependent (or thixotropic) materials which is more relevant to the work carried out in the thesis.

Corvisier et al. [28] studied the flow of thixotropic fluids through pipes. Suspensions of Laponite and Veegum particles were used for their study. Laponite is a synthetic clay with constituent particles in the form of a circular disk of diameter 25 - 30 nm and thickness of 1 - 2 nm, while Veegum comprises particle discs of diameter 400 nm and thickness 4 nm. Both particles

are reported to have a positive and negative charge on the edge and face, respectively, when dispersed in deionized water. Gel formation in these suspensions is attributed to particle aggregation due to positive and negative charges on particle surface in aqueous medium. In the experiments, suspensions (Laponite 2 wt% & Veegum 6 wt%) were prepared and stored for 48 hours and were subsequently loaded into a tank. The suspension was then driven through a pipe with the flow rate set by piston motion (see fig. 2.1 for more details). At the pipe entrance, a filter was installed to break the gel structure by imposing high shear rates (about 500 s^{-1}) before it entered the tube.

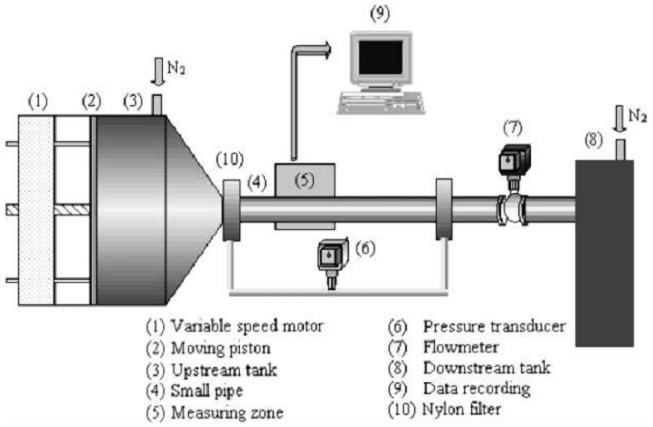

Figure 2.1. Schematic of the experimental set-up for studying pressure driven flow of Laponite dispersions through a pipe. This figure has been reprinted with permission from Corvisier, et al. [28].

The velocities were measured using particle imaging velocimetry (PIV) & ultrasonic velocity profiling (UVP) techniques. In UVP, pulse of ultrasonic sound waves are injected and back-scattered waves from suspended particles are recorded. Particle movement results in shift in phase of waves over time. This allows for calculation of local velocity. In PIV method, tracer particles are added to the suspension and the acquired images are analyzed to obtain the radial velocity profiles. The results exhibited a parabolic velocity profile at the pipe entrance which becomes progressively flat downstream. The flattening or plug like region is pronounced in central region where the shear rate reduces to zero leading to particle aggregation. The size of the plug region increases along the flow length. Similar results were also reported by Oh et al. [29] for non-Brownian suspensions of polystyrene particles in pipes (Diameter = 6.3mm). It was

observed that with an increase in the flow rate, the residence time of the fluid in the middle of the pipe is lowered resulting in slower aggregation process thereby resulting in large difference between average and maximum velocity at the pipe axis.

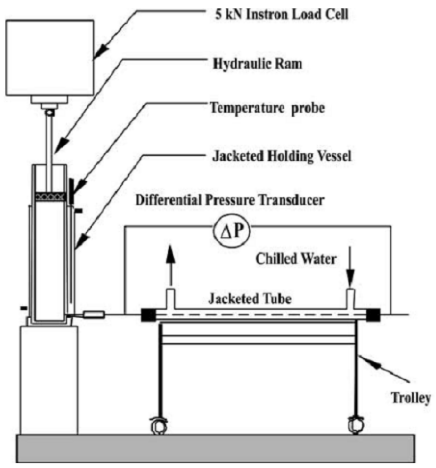

Figure 2.2. Experimental setup for thixotropic fluid flow behavior under different flow rates. This figure has been reprinted with permission from O'Donnell, et al. [30].

O'Donnell and Butler [30] investigated time dependent tube flow of yoghurt, a thixotropic fluid. They stored yoghurt in a holding vessel and flow rate was imposed and regulated using a hydraulic ram (see fig. 2.2). The yogurt was pre-sheared before flowing through the experimental tube. The experiments were performed for a longer duration than average residence time in the tube and pressure drop across the pipe was recorded for different conditions. It was found that the pressure drop increases with flow rate, pipe length and decreasing pipe diameter. The experimental results were compared with power law model based on initial and equilibrium conditions. The initial and equilibrium models, respectively, were only able to capture the pipe flow response (pressure drop at given flow rate) of material at short and long residence time. For better predictions of experimental data at given shear rate, it requires to account tube residence time in the values of power-law indices.

Given the fact that rheological properties of thixotropic material may evolve substantially over period of time, the interpretation of pressure driven flows of such materials can get tricky. This evolution can be attributed to simultaneous microstructure buildup and breakdown during

the flow. The transients within the microstructural changes during pipe flow were investigated theoretically by Cunha, J. P., et al. [31]. The authors considered fluidity (i.e. inverse of viscosity) to describe state of the material which varies between 0 (fully developed structure) to 1 (fully unstructured state) [32]. Input variables to the model were obtained from rheological tests of a model thixotropic material, Laponite suspension in this case. The equations were solved for time dependent flow material in the pipe for different parameters like plastic number (PI = ratio of material yield stress to wall shear stress), initial structuring level and no-slip condition. The values of PI = 1 and PI = 0, respectively, represent a plug state and a sheared state across the entire pipe cross-section [31].

The computations were performed for two different initial states. Starting from a fully unstructured initial state of material, the viscosity increases with flow time leading to reduction of the velocity magnitude. The structure builds up quicker near the center leading to the formation of plug-like region which expands radially over time. The faster build-up at the center can be attributed to lesser shear, thereby possibly reducing structural breakage. The fully developed, steady state flow then represents a plug region over most of the cross-section with a very small region of shear near the walls. The same steady state is reached by progressive de-structuring of the flowing suspension if the initial state is fully structured. The steady state profile reached is, thus, independent of the initial state of the system.

The above mentioned plug formation near the tube center has also been observed for the flow of non-thixotropic suspensions of neutrally buoyant and non-interacting particles by Oh et at [29] for low Reynolds number flows (Re < 1). The suspension was prepared by dispersing polystyrene spheres (size = 40 ± 3 μm) in polymonobutyl ether to achieve a particle volume fraction in the range 0.3 to 0.4. The plug formation near the center is attributed to migration of particles towards the center due to shear. This collection of spheres results in formation of a highly packed assembly of particles which moves as a plug with shearing taking place near the wall comprising a lower volume fraction of particles. The radius or the size of this plug increases with increase in the overall volume fraction of particles in the suspension. The presence of such regions of packed particles and the flow profiles was studied by Oh et al. [29] using MRI imaging technique. The experimental results compared well with compaction model [33] which considered normal stress differences. Similar kinds of non-uniform particle concentration

distribution has also been observed previously in other studies [34-36].

While the formation of central plug-like region seems to exist irrespective of the nature of the suspension during its flow in a pipe, the possibility of its extension up to the pipe wall and its dependence on operating parameters is not clear. Such plug formation across the tube cross-section may completely block the flow thereby leading to sudden rise in pressure drop or it may as well slip along the walls depending on the nature of material. In the next section, we discuss literature studied focused on understanding the wall slip during pipe and channel flow of suspensions. The problems due to complete blockage and necessary measures required to re-start the flow are discussed in a further section.

2.2 Slip in pipe flow

The flowing fluids can be accurately described if the boundary conditions at fluid-solid interface are known. Typically, a no-slip condition is considered at fluid-solid surface. However, liquids can slip at the interface depending on liquid-solid interaction [9, 10, 37]. Poorly wetting surface, i.e. hydrophobic or surfaces with higher liquid-solid contact angles, often result in flow slip [37, 38]. Two mechanisms have been proposed for the slip [39]: True and apparent slip. Apparent slip occurs due to a thin layer (defined mostly for particle suspension system) close to the wall where velocity increases gradually from the solid interface. The layered region refers to high shear flow of different rheological properties than that for the bulk fluid. While true slip (or molecular slip) represents a fluid close to the wall moving with a different velocity than the wall itself.

Few studies have explored the role of the microscopic nature of solid surface that leads to either decrease [40] or increase [41-43] in flow friction, consequently higher or lower slip. It has been accepted that the slip flow deviates from predicted solution using no-slip boundary condition for a capillary flow [44-46], torsion flow [44] and flow between gap of sphere-flat geometry [47]. In recent years, theoretical treatment [48] and advanced measuring techniques have been employed to investigate interface boundary condition which explains the effects of shear rate [47, 49, 50], particle size [51], slip velocity [52] and system size[53, 54] on slip. Slip velocity and slip length are two representative quantities used widely in literature to describe slip. The above studies mainly pertain to flow of Newtonian fluids.

Significant slippage is observed in non-Newtonian fluid flow system [52, 55, 56]. Aktas, et al. [44] have reported the slippage in pipe flow of visco-plastic hydrogel (0.2 wt% Carbopol 940) and compared the results with pure shear flow in absence of slip. The pressure driven flow was studied in a capillary rheometer in conjunction with velocity measurements using tracer particles. Hydrogel exhibits shear thinning characteristics with solid-like behavior under quiescent conditions.

Steady state velocity profiles were measured for various wall shear stress ($\tau_w = \Delta PD/4L$) values, where $\Delta P/L$ is pressure drop per unit length (L) and D is capillary diameter. The flow exhibits a change from complete plug-like regime for τ_w less than material yield stress to a regime comprising central plug and a wall shear zone for higher wall shear stresses (> yield stress). The analytical expressions for velocity profiles and flow rate were derived assuming Herschel-Bulkley fluid (exhibiting yield stress and shear thinning) and a thin layer of Newtonian fluid adjacent to the pipe wall termed as slip region. The slip velocity was found to increase with increasing wall shear stress while the contribution of the slip to the overall flow rate was the highest for a complete plug-like regime. It has been shown that experimental measurements agree with theoretical scaling for the steady state slip velocity expressed in terms of wall shear stress and slip length, even for materials with time dependent rheology.

Similar slip behavior was also observed by Kalyon, et al. [52] for concentrated particle suspensions showing visco-plastic behavior. The work resulted in a non-linear relationship between slip velocity and shear stress. The relation holds for both drag-induced and pressure driven flows. Unlike shear thinning fluid, suspensions exhibiting shear thickening show enhancement in slip with shear stress [56]. Despite fluid rheological properties, there is a wide variation in reported results on slip dependence of super hydrophobic surfaces, with some reports claiming enhancement of slip effects and others claiming diminishing slip effects [57].

While the above mentioned studies provide some insight into slippage for thixotropic fluids, they are not enough to recover simple scaling laws to characterize the slip behavior. This is particularly important as it will allow correlation of the overall behavior with easily measurable variables.

2.3 Startup of blocked pipeline

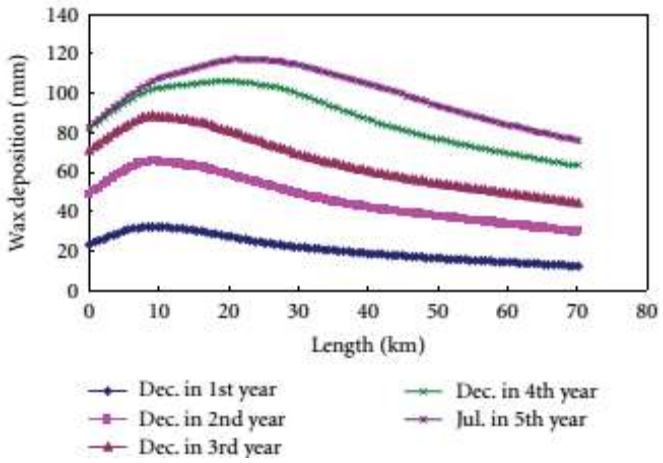

Figure 2.3. Simulated data for wax deposition along the pipeline during normal operation without pigging. This figure has been reprinted with permission from Miao, et al. [58].

The waxy oils typically handled in crude oil industry are thixotropic in nature and they have a tendency to block the entire pipeline due to accumulation of flowing material across the entire cross-section over time. This requires restarting of the flow in a long pipeline, a common occurrence in the crude oil industry. Given that these pipelines are spanned across several geographical regions, the flowing fluid is subjected to varying temperatures. As the temperature decreases, dispersed wax crystals start appearing in flowing crude oil. This temperature is called the wax appearance temperature (WAT). Below the WAT, wax deposits on pipe walls. During normal operation, the ambient temperature, oil flow rate, oil composition, thermal history, etc. are the factors that influence the wax deposition rate [59, 60]. It has been reported that the thickness of the deposited wax grows with time (see fig. 2.3) and is more pronounced at lower temperatures [58, 61]. Deposited wax acts as a heat insulator and reduces heat loss, but it also inhibits flow, thus increasing the pumping pressure. This necessitates a shutdown. During shutdown, the crude oil temperature drops further so that the oil becomes a waxy, gel like thick solid. Once the pipe is filled with this waxy gel, it is challenging to restart the pipeline. Enormous pressure is required to pump out the waxy gel, often well above the pressure rating of the pipes. Pigging is often conducted in order to maintain throughput and for steady operations by removing deposited wax.

Chang, et al. [62] studied the restarting of blocked pipes through simulations. They considered two yield stresses: a static yield stress and an elastic yield stress. An elastic yield stress is defined as a minimum stress above which the crude oil shows plastic behavior while the sample flows like a liquid above static yield stress. They outlined three possibilities, depending upon the initial applied pressure [31, 62, 63].

One possibility corresponds to flow restart without any delay wherein the applied pressure is such that the wall shear stress is higher than the static yield stress of the gelled oil. The flow consists of three regions, viz. outermost region where the local stress is higher than the static yield stress, the intermediate creep region where the local stress is lower than the static yield stress, but higher than the elastic yield stress and the central solid-like core region showing an elastic deformation, as the local stress is lower than the elastic yield stress (see fig. 2.4).

If the wall shear stress is between static yield stress and the elastic yield stress, the flow starts with a delay. Here, only creep and elastic deformation area exist in the pipe initially. Finally, when stress is lower than the elastic yield stress, the flow will not start as the waxy gel plug deforms elastically, leaving the gel structure unaffected by shear.

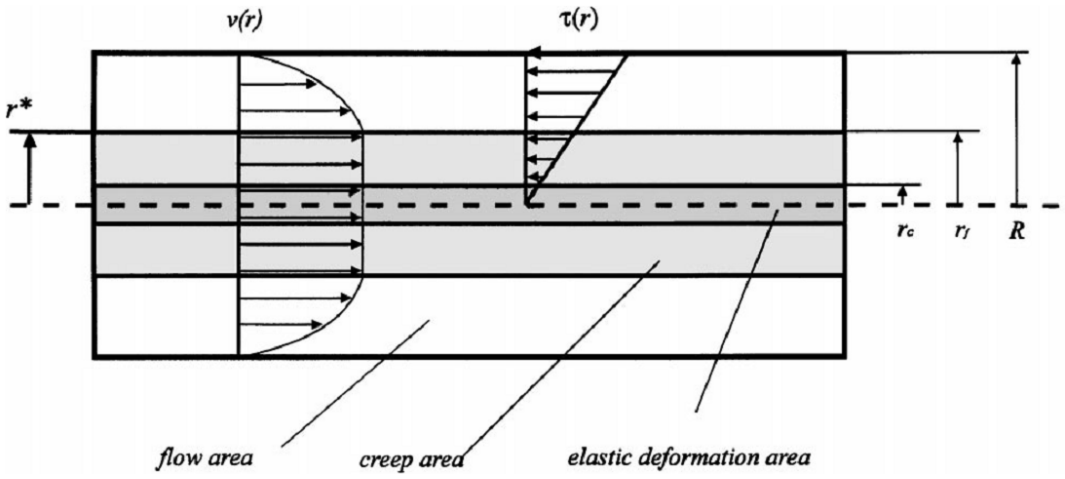

Figure 2.4 Inside flow region of a pipe when flow starts without delay i.e. wall shear stress greater than static yield stress. Flow area $r_f \leq r \leq R$, Creep area $r_c \leq r \leq r_f$ and elastic deformation area $0 \leq r \leq r_c$. This figure has been reprinted with permission from Chang, et al. [62].

During startup, increase in the applied pressure drop leads to increase in the flow rate and

leads to reduction in the delay time for flow resumption. Miao [58] studied the effect of wax deposition thickness and shutdown duration on restart pressure. The wax deposition process during normal operation was modeled considering time dependent aging of material. It was shown that the restart pressure increases with deposited wax thickness and with shutdown duration. Most long duration shutdowns and operation of pipelines without pigging are responsible for increase in the required pressure drop above the design pressure for the pipeline.

Qualitatively similar results have been seen by Cunha, et al. [31], during pressure driven flow of thixotropic model fluid in tubes. Initially, material is considered to be completely structured material state resembling solid rheological properties. They have shown through their mathematical model that material microstructure structure breaks under applied pressure gradient starting from pipe wall, where stress is maximum, to the center. Then the material starts to flow either instantly or eventually depending on intensity of applied stress. The proposed model predicts time dependent microstructural structure properties and captures avalanche phenomenon (unyielded material suddenly starts to flow) during startup [64, 65].

As seen above, the clogging of pipeline and their re-startup poses a big problem for industry and at times necessitates closure of the lines completely. Given that the origin of these issue is the clogging behavior of thixotropic fluids, a deeper insight into the pressure driven flow of such fluids will be of immense usage for such systems.

2.4 Rheology of thixotropic fluids

Contrasting to the pressure driven flows, rheology studies (i.e. in a controlled environment in a rheometer) are quite abundant in literature. The understanding of the rheology of these fluids is, however, quite essential to understand the pressure driven flows and the gel formation and clogging in such fluids. The relation between material properties and shear stress under varying conditions, as gathered from rheology studies, is what is eventually used in elucidating the clogging behavior in pressure driven flows. In the following, we review some of the important literature studies relevant to the thesis work.

Commonly used rheometer geometries include coaxial cylinders (CC), cone and plate (CP) and parallel plate (PP). In each of these, there are rotating and stationary parts. Rheometers are

operated either in a stress control mode or in a strain control mode. In a controlled stress rheometer, the motor torque of the rotating part is independently varied. An angular position sensor measures the movement of the rotating part. The applied torque value is converted to shear stress and position value is converted to strain, considering specific calibration of the in-built sensors. In contrast, in a controlled strain rheometer, the strain on the sample is prescribed using a powerful drive motor and the resultant torque on the rotating part is measured. Typically, the liquids deform with a constant rate for a specified applied force, but solids show a constant deformation that is proportional to the applied force (before the onset of plastic yield). Thixotropic suspensions exhibit time dependent shear thinning behavior, and transform into an arrested state under static conditions.

Oscillatory rheology is also employed to investigate liquid-solid transformation of aging suspension. Elastic modulus (G') and loss modulus (G"), respectively, are measures of elastic behavior of solid and viscous behavior of liquid. In a quiescent state with an oscillatory mode, at early times G' is lower than G" which represents a liquid-like state. With increasing time, G' increases faster than G", leading to a cross-over at long enough times resulting in a solid-like state. The crossover point is called as jamming point [66]. Similar liquid-to-solid variation can also be deduced by variation of G' and G" with oscillatory frequency. In the liquid state, magnitude of G' is lower than G" and it increases slower with frequency compared with G". In the solid state, magnitude of G' is much higher than that of G" and further, G" remains constant with time. The crossover state is represented by a power-law dependence of both G' and G" with frequency with near identical index of 0.5. The crossover point is defined as a gel point (Winter and Chambon [67]) [68].

Coussot, et al. [69] studied aging behavior of thixotropic suspension using a controlled stress rheometer (Bohlin C-VOR200). To avoid wall slip, they used "vane in cup" geometry with a rough surface and a six-blade vane as inner rotating part as shown in fig. 2.5. Thixotropic fluids like Bentonite suspension, mustard and hair gel were used in the study. Bentonite suspension was prepared with particles having high aspect ratio (length: 1 μm) about 100. The particles have positive and negative charges on the edges and the faces respectively. During particle dispersion in the solvent, the stack of particles swells, charges develop on particle surface and finally particles aggregate via edge to face attractive interactions.

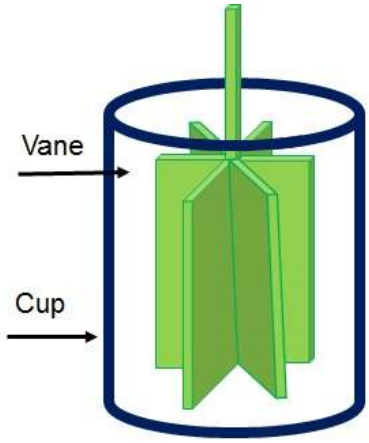

Figure 2.5. Schematic of vane in Couette geometry. In this rheometer, the inner vane rotates and the outer one is held static. The sample is placed in the gap.

The homogenized mixture of Bentonite powder and water was loaded in the rheometer and was allowed to gel. Each sample was pre-sheared at a high shear rate to generate a uniform, well-defined initial condition for the experiments. The evolution of strain was then recorded for constant stress conditions. Two regimes were observed. For small enough stress, the strain increased a little for a short duration before reaching a plateau suggesting a solid-like behavior. For high enough stresses, the strain evolves continuously suggesting a liquid-like behavior. A transition regime is observed for intermediate stress values. In a later study, Ovarlez and Coussot [66] explored the effect of temperature and concentration for the same system. A rapid jamming is observed with increase in temperature due to increase in particle collision and with increasing particle concentration due to particle crowding.

The liquid-solid transition was explored in more detail by Ovarlez and Chateau [70] using standard Couette geometry by measuring the time evolution of elastic modulus (G') and strain across the transition point. Suspensions of three materials, Bentonite, mustard and silica, all showing thixotropic behavior were considered. The samples were pre-sheared rapidly to create a liquid-like initial state. The sample was, then, subjected to a zero stress (quiescent state) and a higher stress. In both cases, G' showed a continuous increase with time. The increase was gradual during quiescent state, while there was a sudden jump in the value of G' in second case. The authors considered the rapid jump to be a liquid-solid transition point. The value of G' was nearly zero in the latter case during pre-transition period while it jumped to a much higher value than that for

quiescent state post the transition period. The authors also found qualitative as well as quantitative differences for the evolution of strain. In the pre-transition period, the strain increased linearly with time, while it remained constant post the transition point. The time to achieve the plateau in strain values, however, increased with increasing applied stress. For the applied stress larger than critical stress, the time to reach transition extends to infinity.

Coussot, et al. [71] also studied the effect of rest time on the rheology of thixotropic suspensions. A "vane in cup" geometry was used to eliminate slip. After pre-shearing the sample was allowed to rest for different resting times. A constant stress was then applied on each of the samples and viscosity was recorded with time. The sample is found to increasingly age with rest time leading to progressively higher values of viscosities. However, on shearing, the viscosity reduces and converges to a constant value. However, beyond a critical rest time, the viscosity of the sample actually increases with shearing time suggesting a formation of structure which is strong enough to be broken due to applied shear.

Apart from complex rheological properties, shear banding phenomenon is seen in processing of polymer melt [72], suspensions [73] and molten metal [74]. During flow processing, material structure formation and breakage tendency in response to shear rate vary along the flow cross-section. Structure buildup at low shear is much faster than the high shear rate region. Thus, there is discontinuity in material state which leads to dissimilar flow regimes (coexistence of high and low shear rate flow regions side by side). In polymer processing, the phenomenon often induces surface instability. However in time dependent material flow system, shear banding effects diminishes at steady state and it shows continuous material state coexisting plug-shear flow [32].

The above mentioned studies seem to provide a reasonable understanding about liquid-like, solid-like behaviors of thixotropic fluids and the transition between the two captured very well in terms of rheological parameters. Exact application of these results to actual transition and clogging behavior in pipe flows, however, remains unclear.

2.5 Conclusions

The pressure driven flow of thixotropic fluids through capillaries or pipes is often accompanied by time dependent flow resistance. This owes its origin to the material time dependent ageing

behavior due to inter-particle attraction leading to formation of sample spanning clusters which block the flow area. Such block formations often exhibit slippage with respect to the pipe wall owing to the wall-fluid interaction or due to material properties itself. Excessive clustering or ageing can block the flow completely, typically seen in oil pipelines which provides several problems in flow restarts and requires special measures for the same. The above mentioned behaviors are governed by the complex rheology behavior of such materials which, at laboratory scales, shows very interesting dependence on material preparation and shearing protocol in addition to the material properties and concentrations. Successful design and operation of pipe flow of suspensions require comprehensive studies correlating above distinct behaviors either through elaborate theoretical studies or through simple correlations based on system variables.

Based on the review provided in this chapter, we envisage following research problems that can be pursued to address the gaps present amongst various literature studies

1. Experimental study of transient flow behavior of model ageing material in pipes subject to various material properties and operating variables
2. Determination of simple scaling relations for flow of thixotropic materials in pipes to provide predictive abilities
3. Microstructural evolution and its correlating with partial and complete blocking of flow for various applied pressures and pipe dimensions.

The specific objectives of the thesis work are

1. Design experimental system and methodology for the pipe flow study of time dependent material.
2. Study in-situ flow blocking behavior and transient behavior of time dependent suspension during pressure driven flow through a tube.
3. Experimental investigation of dependence of parameters such as pipe diameter, pipe length, time scale associated with material properties, flow rate, etc. during flow of material through a pipe.

Chapter - 3

3 Experimental Methodology

For study of pressure driven pipe flow of thixotropic fluids the choice of model fluid type and design and fabrication of the entire experimental system are the most critical factors to be considered. The model fluid is required to exhibit time dependent properties, should be well characterized in literature in terms of its rheological properties and should be easy to handle. The system design is dependent on the type of fluid and its time dependent characteristics which should be accounted for appropriately while measuring the flow properties. In this chapter, we provide a detailed account of the design of experimental system, the issues involved therein on account of the type of model fluid chosen, progressive system modifications, characteristics of the model fluid and experimental procedure to acquire flow characteristics of relevance.

3.1 Model fluid

The suspension of LAPONITE® clay particles is considered as a model thixotropic fluid in current research work. This material is very well studied in literature and exhibits significant time dependence and ability to span the sample or system, thereby making it a suitable for studying flow and clogging behavior. In the following, we provide details about LAPONITE® clay and its characteristics.

LAPONITE® is a synthetic hectorite clay and is used widely as a rheology modifier, film former, in various personal care products, coatings applications, ceramics and pharmaceutics products. The individual clay particle is disk shaped with large aspect ratio (defined as particle diameter to thickness having an approximate value of 27) (see fig. 3.1a.). The LAPONITE® crystal is composed of an octahedral magnesia layer which is sandwiched between two tetrahedral silica

layers on either side having chemical formula $Na^{+0.7}[(Si_8Mg_{5.5}Li_{0.3})O_{20}(OH)_4]^{-0.7}$. The disk shaped particles, in a dry state, are present in the form of aggregated particle stacks. Upon dispersing LAPONITE® powder in water, these aggregated stacks separate into individual stack of LAPONITE® particles (see fig. 3.2). Further, water enters between platelets space causing them to swell [75] leading to dissimilar +ve and –ve charges on circular rim and face, respectively. The charged particles interact with each other via attractive edge-face and repulsive face-face interactions, leading to possible particle-particle aggregation via face to edge attraction [76, 77] thereby resulting in a 3 dimensional network percolation of aggregates [78] (see fig. 3.1b). In dispersed phase, particles experience long range repulsion between the faces of particles and short range attraction between the edges and the faces of platelets [79]. The addition of salt like NaCl, KCl, $Ca(Cl)_2$, to the dispersion effectively reduces inter-particle repulsion by screening surface charges of particles [80, 81] and enhances aggregation tendency.

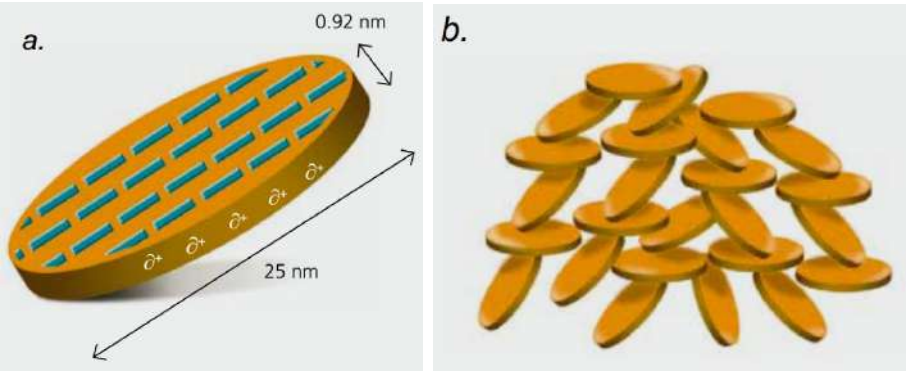

Figure 3.1 Schematic representation of (a) disperesed single LAPONITE® crystal with associated charges on surface and (b) aggreagated structure of LAPONITE® particles in suspension. This figure has been reprinted with permission from BYK Additives & Instruments [82].

The aqueous dispersion of (colloidal) LAPONITE® particles exhibits time dependent microstructural evolution in quiescent state as well as in sheared state. In quiescent state, the microstructure evolves over a period of time resulting in gradual rise in elastic and viscous modulus. Thus, the rheological behavior is due to microstructure build-up or physical aging which transforms a liquid like state (negligible elastic modulus value) into an arrested or a solid like state (with a high elastic modulus). The suspension of Laponite particles has been claimed to exhibit various phases: gel, attractive glass, Wigner glass, Nematic phase, Sol phase, etc [76, 83] reported

in literature and classified in the phase diagram created using two variables, viz. ionic strength of added salt and concentration of LAPONITE®. With increased salt concentration, the suspension goes from a repulsion dominated state to an attraction dominated state with further phase separation due to excessive screening of surface charges. The rate of transition of arrested phase increases rapidly with increasing ionic strength [81] and further decreases with ionic strength upon excess addition of salt [84]. Similarly, the mechanical properties are observed to be enhanced with increasing clay concentration due to reduction of electrostatic repulsion [84-86]. The classification or distinction between the gel-state and glassy-state of remains unclear, but the suspension can undergo solid like transformation at LAPONITE® particle volume fraction as low as 0.004.

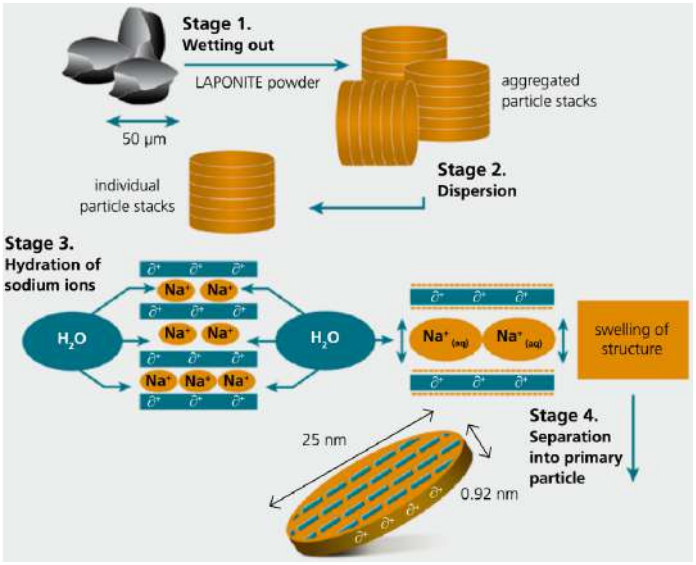

Figure 3.2 Various stages of dispersion process of LAPONITE® powder in aquaous medium. This figure has been reprinted with permission from BYK Additives & Instruments [82].

On the other hand, application of shear reverses the aging process due to breakdown of microstructure. This phenomenon is called as shear melting or shear thinning. Typical characteristics of LAPONITE® suspension like transition from freely flowing liquid state to soft solid phase [87, 88], slowly forming microstructure to rapidly aging dynamics [89], structuring to de-structuring phenomenon [90, 91] etc. are observed in rheological studies. In addition to extensive rheological studies, few studies have focused on studying the flow behavior of

LAPONITE® suspension through pipes with respect to the transient behavior, equilibrium flow properties and flowability [28, 31, 92].

3.2 Materials

LAPONITE® (of XLG grade) was obtained from BYK additive, Japan. For every experiment, LAPONITE® powder is first dried at 120 ^{o}C for 4 hours to remove moisture and is then maintained at 50^{o}C and used in experiments as required. NaCl salt (procured from Merck Specialities Pvt. Ltd. Mumbai) is used to modify the suspension ageing behavior. The suspension was prepared using de-ionized (DI) water as obtained from a Millipore system (pH = 7, conductivity = 18.2 µS/cm). Fluorescent polystyrene (PS) latex particles of size 1.08 µm with a polydispersity of 4 % from Micro-particle GmbH, Germany were used as tracer particles for flow visualization studies. Silica particles of 1 µm size, obtained from Richen Laboratories, Hong Kong, were used for micro-rheological studies. The pressure measurements were obtained using a manometer, pre-filled with paraffin liquid of viscosity 17.3 cSt and density 0.83 g/cm^3, purchased from Alpha Chemika, Mumbai. Red color food dye and blue color ink were obtained from NAISA Colour Co. Ahmedabad and Kirpal Industries, Indore, respectively.

3.3 Experimental system

Experiments were carried out in batch mode as well as continuous mode operation. In the former, a fixed amount of LAPONITE® suspension was prepared and drained out steadily over time to flow through a pipe. In the latter, a fixed amount of material was maintained in a vessel in the mixed state with a fixed amount being drained over time which is exactly equal to the amount being added to the mixture. The issues faced during the experimentation, the relevant resolutions and evolution of the final experimental system are discussed in the next few sections.

3.3.1 Experiments in a batch mode

The schematic of the experimental system is shown in figure. 3.3. Predefined amount of dry LAPONITE® powder was added to a vessel containing aqueous solution of NaCl of prescribed concentration. The mixture was stirred by a homogenizer (IKA T25 digital Ultra-Turrax) at high

speed (4000 rpm) to ensure complete dispersion of powder within 30 minutes. The stirring was maintained at constant speed throughout the experiments to prevent the suspension from ageing. The rotational speed of the stirrer was adjusted so as to prevent significant turbulence that may cause air bubbles to get entrained in the mixture. A few experiments were also tried with a magnetic stirrer (IKA), which, however, was not efficient enough to prevent ageing of the suspension adequately due to limitations on rotational speed range. The temperature of the mixture was maintained at a constant (room) temperature using a water bath.

The mixed suspension was pumped to the inlet of a pipe using a peristaltic pump at a fixed flow rate. The pipe was pre-filled carefully with the mixed suspension of same concentration to avoid trapping of air bubbles inside the pipe. A flexible, small (diameter of 0.1 cm) silicone tubing was used to transfer suspension from the mixing vessel to the pipe. The small size and shorter length (25 cm) of the tubing ensures minimum structural changes in the state of the suspension state during fluid flow. The exit of the pipe was left open to atmosphere.

A manometer (HTC PM – 6205, Mumbai) with measurable range of 35 kPa was used to measure pressure drop across the length of the pipe. A plastic tube connecting the flow line to the manometer diaphragm sensor was filled with a low viscosity (17.3 cSt) paraffin oil, sensitive enough to transmit small pressure fluctuations as well as immiscible with the aqueous suspension. The constant flow condition through the pipe was ensured by measuring the outflow from the pipe at regular intervals.

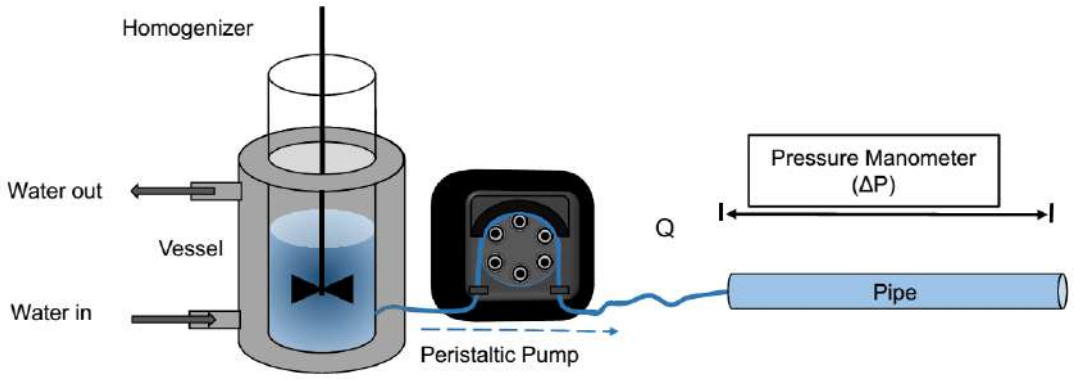

Figure 3.3. Experimental setup for the study of LAPONITE® suspension flow through a pipe in a batch mode.

The experiments performed in the batch mode, however, exhibited certain following non-resolvable issues, viz. (i) unsuitability for a longer duration experiments due to finite volume in the vessel, (ii) state of the suspension varies with time in spite of continuous stirring (discussed in sec. 3.4.2.3) and (iii) limitations in exploring a wider range of operating parameters like pipe diameter, pipe length, flow rate and concentrations of LAPONITE® and salt, due to small operational window. To overcome these limitations, the experiments were performed in continuous mode as described next.

3.3.2 Experiments in continuous flow mode

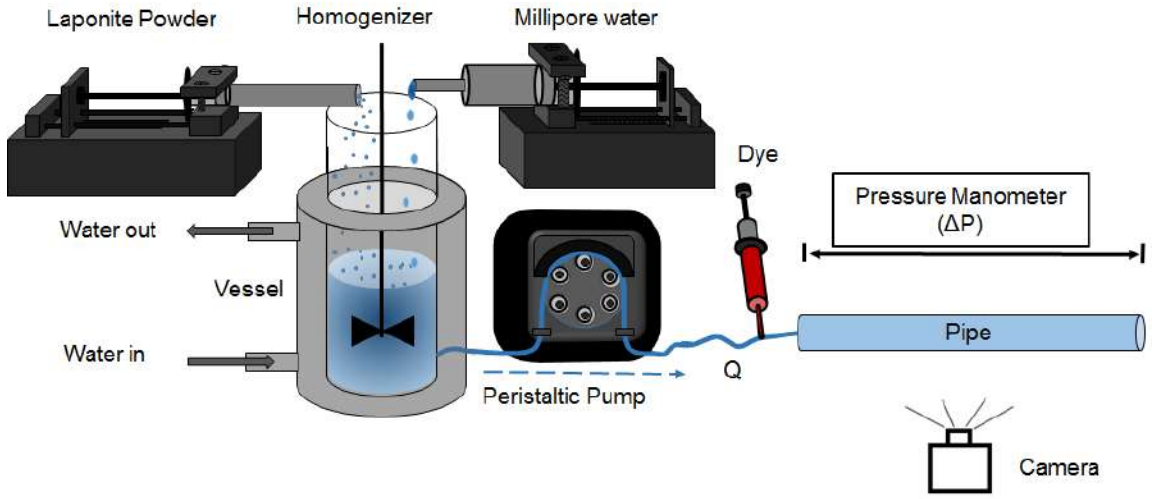

Figure 3.4 Schematic of continuous flow process for LAPONITE® suspension preparation.

The experiments in continuous flow mode comprised continuous addition of powder and NaCl solution, each separately, into a mixing vessel as shown in the schematic (see fig. 3.4). Initially, LAPONITE® suspension of desired concentration is prepared in a tank by vigorous stirring at high speed (4000 rpm) for 30 mins using a homogenizer (IKA T25 digital Ultra-Turrax). Then, aqueous NaCl solution and dry LAPONITE® powder are added continuously into the tank at constant rate using a syringe pump while being stirred continuously at 4000 rpm using the homogenizer so as to maintain the desired concentration throughout the experiments. Simultaneously, the suspension from the vessel is pumped to a pipe. The flow rate into the vessel (q_{in}) and out from the vessel (q_{out}) are identical to maintain constant volume in the vessel with the average residence time

(V/q_{in}) of 45 minutes maintained for all the experiments, where V is the volume of suspension in the mixing vessel. All the mass flow rates set by peristaltic pump and syringe pump are verified by collecting material over a period of time (see section 3.4.1 for more details). The continuous flow methodology ensures constant the state of the LAPONITE® dispersion throughout the duration of the experiment. This was verified by measuring mass flow rate at the outlet from the vessel which remained constant in time (see section 3.4.2.4 for more details on these measurements).

The LAPONITE® suspension, is pumped from the mixing vessel into a pipe prefilled with water. The suspension, thus, displaces the water in the pipe over a time duration corresponding to the flow rate and the tube diameter following which pressure drop measurements were recorded. The pressure drop across the pipe length allowed for inferences on the state of the flowing suspension in the pipe. Few experiments were carried out with the pipe pre-filled with LAPONITE® suspension having same concentration as that in the vessel (refer appedix A for further details). However, the presence of LAPONITE® suspension in quiescent state in the pipe before actual flow starts resulted in its ageing which then mixed with the incoming fresh suspension, precluding studies of the exact effect of flow on suspension behavior.

Experiments were carried out with pipe having tapered entry and a flat exit (see appendix A for further details). The tapered entry allowed for a smoother flow into the pipe due to gradual increase in the flow cross-section. On the other hand, a flat exit minimizes any resistance to the outflow of any supposedly solid-like structures formed within the pipe due to inherent ageing tendency of LAPONITE® suspension. The latter inference was validated during few preliminary experiments carried out with a tapered exit. The measured pressure drop values in this case showed dramatic fluctuations, which most likely seem to be associated with the non-uniform (squeezing) exit of possible solid-like structures from the tapered exit. There are several other issues encountered during system design which are elaborated in more detail in appendix A.

In the entire study, we have used suspension with varying LAPONITE® concentrations (1.6, 1.8, 2.2, 2.4, 2.8 and 2.9 wt%) and salt concentrations (3 and 6 and 9 mM). The DLVO theory suggests that the energy barrier for attractive interaction decreases with increase in salt concentration. Varying salt concentrations, thereby, allows to study the effect of changing particle interaction on the overall flow behavior. Glass tubes (lengths 15.5 cm and 30 cm each with an

internal diameter of 0.4 cm and 0.72 cm) and steel tube (length 23 and 53 cm each with an internal diameter of 0.1 cm) were used as pipes. The temperature in the tank was maintained at 25°C throughout the experiment.

3.4 Characterization of different experimental stages

The overall work did involve detailed characterization and subsequent design of various components (pumping systems, flow devices, mixing assembly etc.) to evolve to a final experimental system which ensured consistent experimental data acquisition corroborating with the ensuing physical phenomena. In the next few sections, we deliberate on the characterization and operation of various experimental system components.

3.4.1 Material pumping assembly

Both, LAPONITE® powder and aqueous medium (with or without salt) was added separately as well as continuously to the vessel where the mixing was carried out using a homogenizer.

3.4.1.1 Powder flow system

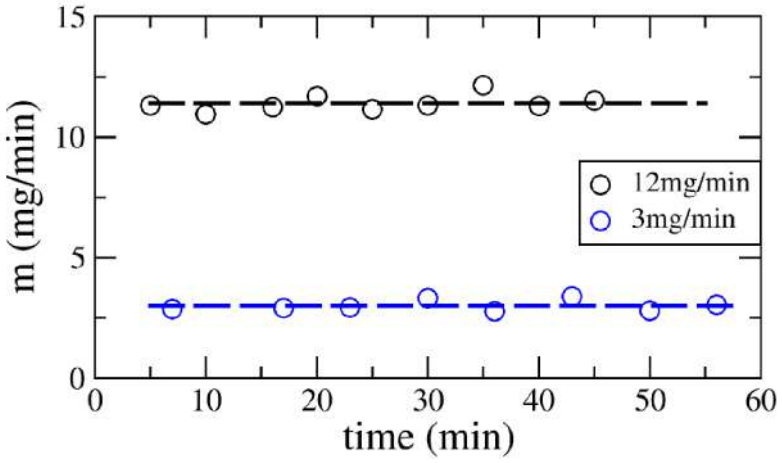

Figure 3.5 Measured mass rate of dry LAPONITE® powder set by syringe pump. Dash line represents average mass rate and different experimental mass rate are represented by different colors.

The powder was pumped at a flow rate of 12 mg/min through a syringe (diameter 4.5 mm and length 70 mm) using a syringe pump (Holmarc HOSPLF-2). The diameter of the syringe was large enough to prevent clogging during the powder flow. The accuracy of the prescribed flow rate, as set by the pump, was verified by weighing the mass of the material collected at the outlet of the syringe with time. Above figure 3.5 shows the variation of the mass flow rate, as measured at the syringe outlet, with time for two different rates (3 mg/min and 12 mg/min) as set by the pump. The flow rates are nearly constant in time and also corresponds to the values set by the pump.

The outlet of the syringe was kept sufficiently above the free surface of the mixture so as to prevent it from getting wet from the splashing of liquid from the mixing vessel and cause clogging. Further, the internal diameter (4 cm) of the vessel and the fill level of liquid (about 4 cm) was finalized to ensure uniform spatial mixing (observed visually) using stirring speed less than 5000 rpm. The mean residence time of the suspension in the mixing vessel was fixed at 50 minutes to prevent ageing of the sample in the vessel over long durations.

3.4.1.2 Aqueous salt/ water addition system

The aqueous medium, either salt solution with prescribed concentration or water, is pumped into the vessel using another syringe pump (Holmarc HOSPLF-2) mounted with a 60 ml syringe. As for powder flow, the outflow rate of the aqueous medium was verified by measuring the outflow of liquid and comparing with the prescribed rate by the pump (data not shown). The flow was quite smooth compared to that of powders.

3.4.1.3 Peristaltic pump

All the experiments were performed under constant flow rate conditions. The stirred suspension in the vessel was pumped to the pipe using a peristaltic pump (Miclins pp 10 EX) allowing flow rate range of 0.1 ml/hr - 1000 ml/hr. A flexible tubing (length 5 cm) connected the pump outlet to the pipe. The pump is composed of movable rollers, stationary plate and a flexible tube sandwiched between moving rollers and stationary plate. It transfers liquid by alternating compression and relaxation of the tube when roller moves over the flexible tube. The pump feedback to the change in the flow behavior within the pipe was ascertained by (i) allowing the liquid to flow through a constant cross-section pipe and (ii) pinching the intermediate tube while blocking the flow. The former case, resembling a flow without clogging, led to a constant pressure drop. The latter case,

resembling flow clogging, led to a sudden rise in pressure leading to back flow. An excessive stoppage duration can cause rupture of the tube connections in the experimental system bursting of the experimental system. This test, thus, allowed us for an intuitive understanding of the pumping system subject to the experimental material being handled.

3.4.1.4 Pulsation dampener

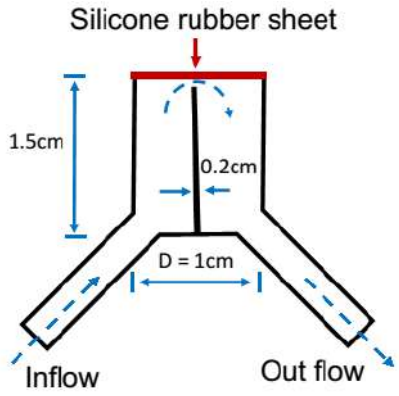

Figure 3.6 Design of the pulsation dampener to minimise pressure fluctuations.

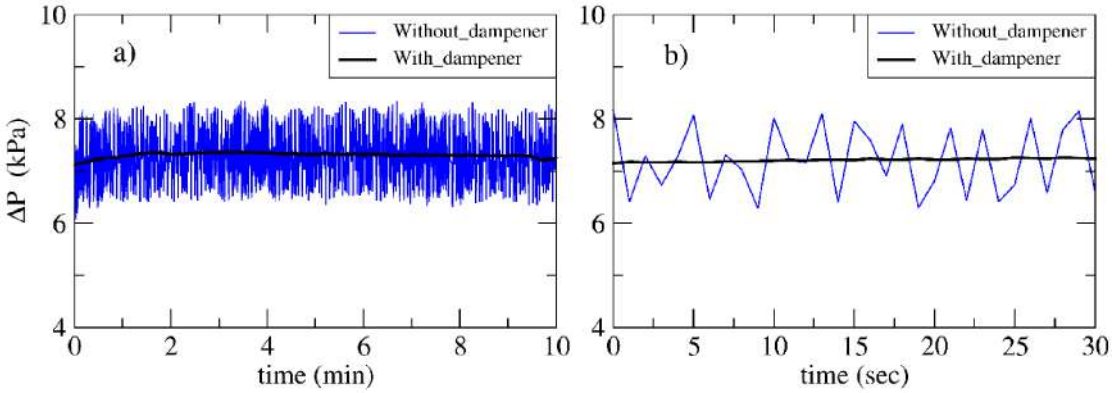

Figure 3.7 Measured pressure difference of flowing PDMS through a circular channel (D = 0.1 cm and L = 24 cm) at a fixed flow rate (0.42 cm^3/min) with and without use of the dampener connected upstream: a) Time dependent pressure drop over 10 minutes b) Magnified view showing the effect of the dampener. The peristaltic pump has a period of about 17 s.

The inherent design and operation of the peristaltic pump causes pressure fluctuations in the flowing fluid. These fluctuations superimpose on the actual pressure drop experienced by the fluid

flowing through the cylindrical tube. To minimize these fluctuations, the outflow from the peristaltic pump is passed through a customized dampener, the schematic for which is shown in figure 3.6. It comprises of a chamber (diameter: 1 cm, height: 1.5 cm & partition width: 0.2 cm) made from polypropylene and fixed with an inlet and an outlet. The fluid from the peristaltic pump flows in to the chamber which is closed from above with a silicone rubber sheet. The pressure fluctuations in the entering fluid get damped due to the presence of rubber sheet and the chamber capacity (150 x 10^{-3} cm^3). This fluid, with minimized pressure fluctuations, then flows from the chamber towards the cylindrical tube.

The performance of the dampener was tested by flowing PDMS fluid (viscosity: 10^{-3} Pa s and density: 0.98 g/cm^3) through a circular pipe of diameter 0.1 cm and length 24 cm. The variation of the measured pressure drop across the length of the channel without dampener is compared with installed dampener shown in figure 3.7. As clearly observed, the fluctuations in the measured pressure are in the range of 6 – 8 kPa during the pumping of PDMS (blue line on fig. 3.7 a and b).These fluctuations are reduced significantly (in the range: 0.1 kPa) after PDMS is passed through the dampener (as shown with black line in fig. 3.7 a and b) before it enters the pipe.

3.4.2 State of suspension outflowing from the vessel

The sole purpose of carrying out experiments in continuous mode was to ensure that the state of the suspension was maintained the same throughout the experimental time duration by stirring the suspension efficiently. This did not seem feasible in a batch experiments as discussed earlier. Different techniques were implemented to ascertain the state of the suspension outflowing from the mixing vessel. We provide details of these methods and their outcomes in the following few sections.

3.4.2.1 Viscosity measurements

One way of ascertaining the state of the suspension is through measurement of its viscosity. A simple "falling sphere" method was used for estimating the viscosity. The velocity of the sphere falling under gravity through the suspension increases and reaches a steady state value known as "terminal settling velocity". The viscosity of the suspension is then given by Stokes law as follows [2]

$$\mu = \frac{2}{9}\frac{(\rho_s - \rho)g{R_s}^2}{V} \tag{3.1}$$

where, μ, V, ρ, ρ_s, R_s and g are, respectively, the viscosity of fluid, terminal settling velocity of falling sphere, density of fluid, density of sphere, radius of sphere and acceleration due to gravity.

The suspension sample was collected from the stirring vessel at different times and places in a transparent square cuvette of dimensions 1 cm x 1 cm x 4 cm. Glass bead of density 2.5 g/cc, used as a sphere, was carefully placed just above the free surface of the suspension in the cuvette and its downward motion was captured using a digital camera (Sony DSC-HX20V). The sphere position at different times (i.e. different distances from free surface), identified using freely available centroid algorithms, was used to obtain the velocity. Experiments were carried out with glass beads of different sizes, 280 µm, 460 µm, 480 µm and 500 µm. It was, however, not possible to obtain consistent enough data for different sphere sizes and samples collected at different times. The velocities never reached a steady state in some cases while its spatial dependence did not follow the standard behavior as expected for a sphere falling in a liquid. Due to this lack of consistent behavior, it was not possible to estimate the viscosity accurately enough, hence the state of the suspension at different times of stirring. We believe that this consistency owes its origin to the highly heterogeneous nature of LAPONITE® suspension and its tendency to undergo microstructural changes in quiescent state. The presence of a distinct microstructure and its time dependent evolution seems to influence the downward motion of the sphere thereby giving rise to inconsistent velocity data [93]. Any further increase in sphere size was not feasible due to possible confinement effects on the overall behavior.

3.4.2.2 Rheology measurements

The rheology measurements involved collecting the suspension outflowing from the vessel at different times and subjecting it to creep measurements in a parallel plate geometry of the rheometer (Anton-Paar, physica MCR 301). Essentially, this involves studying the strain behavior of the sample when subjected to small, but constant stress. The time evolution of the strain for a constant applied stress (1 Pa) for suspension samples collected at different times and for two different concentrations are shown in fig. 3.8. For all the samples, the strain first increases linearly followed by a plateau at long enough times. The plateauing represents evolution of the sample to a solid-like state with an elastic modulus. While the state of the suspension at different times

remains nearly the same for LAPONITE® concentration of 2.7 wt%, it does seem to change dramatically with time for a higher concentration (2.9 wt%). Now this may indicate that the suspension state is changing during preparation. However, it is also to be noted that there is a unavoidable time lag of about ten minutes between collecting the sample from the experiments and transferring it in a rheometer in addition to the time period of near quiescent state during compliance measurements. It is known that LAPONITE® suspension ages under quiescent conditions, the tendency of which increases with LAPONITE® concentration. In view of this, it is difficult to conclude whether the deviations observed for 2.9% salt concentration (fig. 3.8ii) are due to inhomogeneous mixing during preparation or ageing taking place during rheology characterization. We, thus do not consider these measurements a true test of the state of suspension and have reverted different types of measurements.

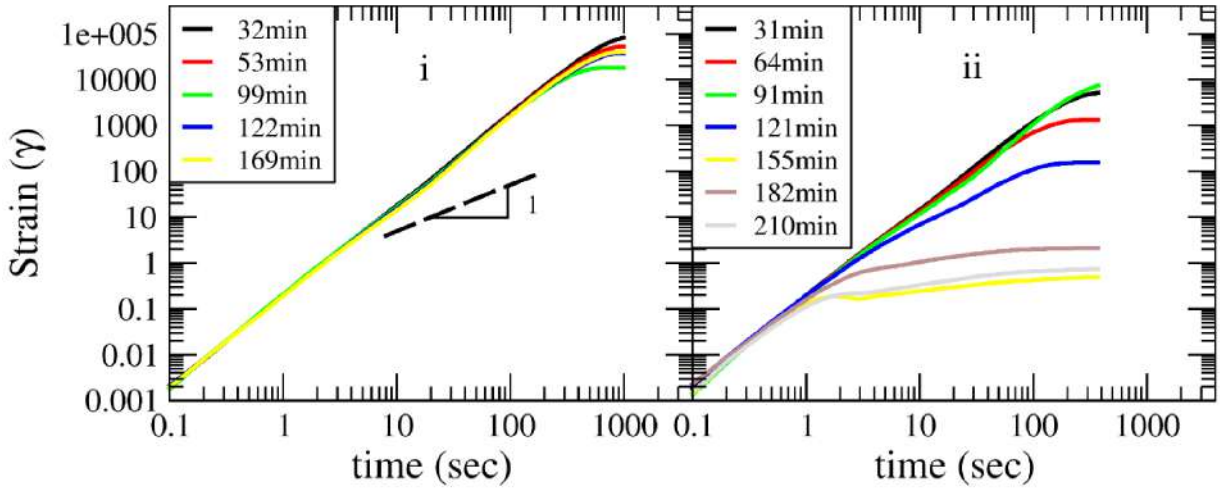

Figure 3.8 Sample compliance response under constant applied stress of 1Pa is plotted as a function of time for two different concentraion of LAPONITE®: i. 2.7 wt% and ii 2.9 wt% . Here different color line indicates sample collection time (t_a).

3.4.2.3 Micro rheology measurements

This technique studies the motion of the tracer particles embedded within the suspension. In the absence of any external force, the tracer particle moves randomly within the suspension (driven by thermal motion) while exploring the space available. For a liquid, the tracer particle exhibits a diffusive behavior while for a gelled (or solid-like) state it exhibits a sub-diffusive behavior. The

rheology at the local level is obtained by converting the tracer particles' displacements to rheological constants. This technique has been routinely used for studying colloidal systems for several years [77-80].

A few milligrams of 1 micron sized silica particles were added to the mixing vessel and stirred along with aqueous LAPONITE® suspension. The outflow sample from the pump outlet was collected at different times (t_a). The sample was loaded in a cavity on the slide and the cavity was sealed carefully with a cover slip to prevent (i) formation of air bubbles (ii) solvent evaporation and (iii) convection. The quiescent sample was immediately observed under a fluorescence microscope (Carl Zeiss Microscope) in bright field mode using 40X objective lens and imaged over a duration of 60 sec (Δt) at a frame rate of 20 frames/sec. It is to be noted that unlike the method discussed in previous section, the time delay between collecting samples and actual visualization is reduced as much as possible so as to prevent change of the state of suspension during this time period, thereby allowing for a possible reliable signature of the state of the suspension.

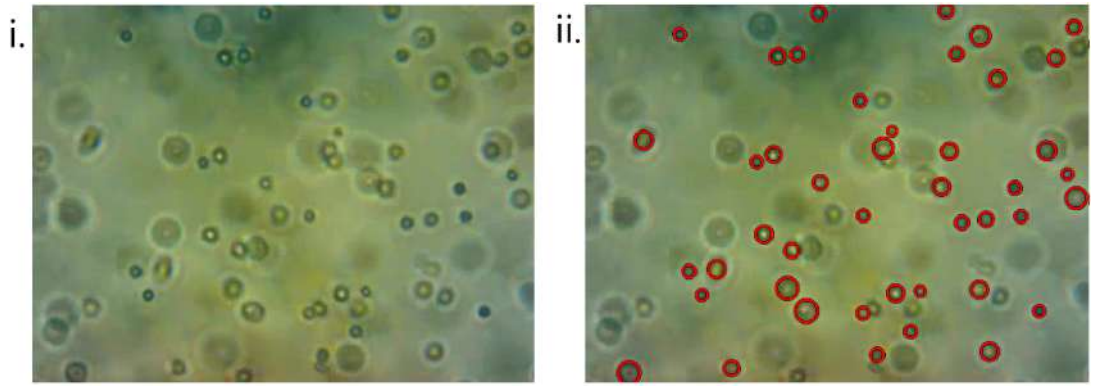

Figure 3.9 i. Microscopic image of suspended silica particles is captured in bright field mode. ii. Particles detected by edge detection method are superimposed on original image. Red circles show detected particles. Big circular spots represent out of focus particles.

Figure 3.9i shows the tracer particles. Due to lack of accurate control over the depth of imaging we see (a) small and sharp circles representing particles in a focused plane and (b) large and blurred circles representing particles out of focused plane. The centroids of focused particles are obtained using freely available centroid algorithm (Crocker & Weeks [94]) which are then

tracked to obtain individual particle trajectories using IDL programming. The mean squared displacements ($\langle \Delta r^2 \rangle$) are obtained from particle trajectories in (x, y) plane as ($\langle \Delta r^2 \rangle = \langle [x(t+\Delta t) - x(t)]^2 + [y(t+\Delta t) - y(t)]^2 \rangle$) where Δt is the lag time. The motion of the particles in z-direction could not be tracked and was, thus, neglected.

Figure 3.10a shows mean squared displacements of the tracer particles in the samples collected from continuous process. The behavior is nearly the same for the samples at different times suggestive of the fact that the state of the sample remains consistent over this time duration. The stirring of the suspension at 4000 rpm carried out using the homogenizer, thus, seems to be sufficient enough to maintain the state of the suspension throughout the experimental run. Further, the mean squared displacements exhibits a power-law dependence on time, with the exponent nearly 1, indicating a purely diffusive behavior reflective of liquid-like behavior. On the contrary, the batch like process reflects a diffusive behavior only for sample taken initially. At later times, the exponent is nearly zero indicating a sub-diffusive behavior typically observed for a gel-like or a solid-like material. The state of the sample is, thus, not consistent for the batch process thereby justifying the need for continuous process in the experiments.

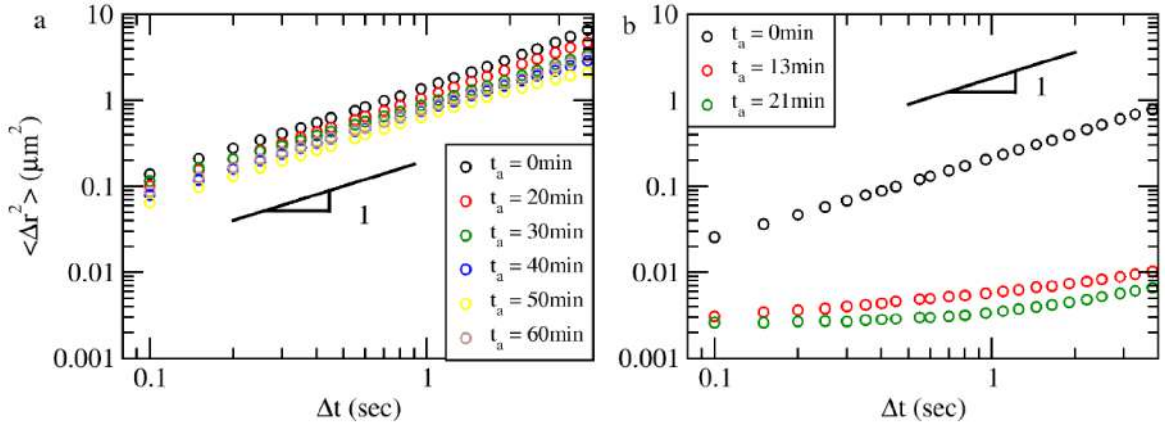

Figure 3.10 Varition of MSD (mean square displacement) as a function of lag time for various aging time (t_a) of LAPONITE® suspension ($C_{laponite}$ = 2.9 wt%, C_s = 3 mM) prepared by a) continuous flow process and b) Batch process under constant stirring speed at 4000 rpm. Different color represents different aging time of suspension.

3.4.2.4 Tube viscometer Pressure measurement

Given the inadequacy in ascertaining the state of the suspension using "falling sphere" technique and contradictory inferences in the other two techniques (bulk and micro rheology), we reverted to measuring the variation of pressure drop with the flow rate to know the suspension state. This method also seems more relevant given that these are the primary measurements made in this entire work.

The suspension from the vessel is passed through a test pipe with diameter (D = 1 cm) and length (L = 21 cm) connected by a small tubing to the vessel. The pressure drop across this test pipe was recorded for a range of flow rates and two different LAPONITE® concentrations at fix salt concentration (3 mM). The time variation of pressure drop and flow rate is shown in fig. 3.11. The flow rate remains constant throughout while the mean pressure difference remains constant throughout with fluctuations. The fluctuations are due to absence of dampener in this case. As mentioned in section 3.4.1.2, these fluctuations get removed substantially after using the dampener. Assuming, Poiseuille flow for a power-law fluid, with exponent "n", the pressure difference (ΔP) varies with flow rate (Q) as [3]

$$\frac{\Delta P}{L} \propto Q^n / D^{1+3n} \tag{3.2}$$

For a constant tube diameter and length, the constancy in the values of ΔP and Q with time suggests a fixed value of the exponent "n", i.e. a constant state of suspension. The measurements, thereby, indicate that the experimental protocol keeps the suspension state nearly constant for the entire experimental duration. Moreover, as described in next section, the final experiments were conducted with only LAPONITE® in the mixing vessel with salt added downstream. In the absence of the salt and low LAPONITE® concentration, the ageing is anyway expected to be minimal and so the concerns about the state of suspension will almost be non-existent.

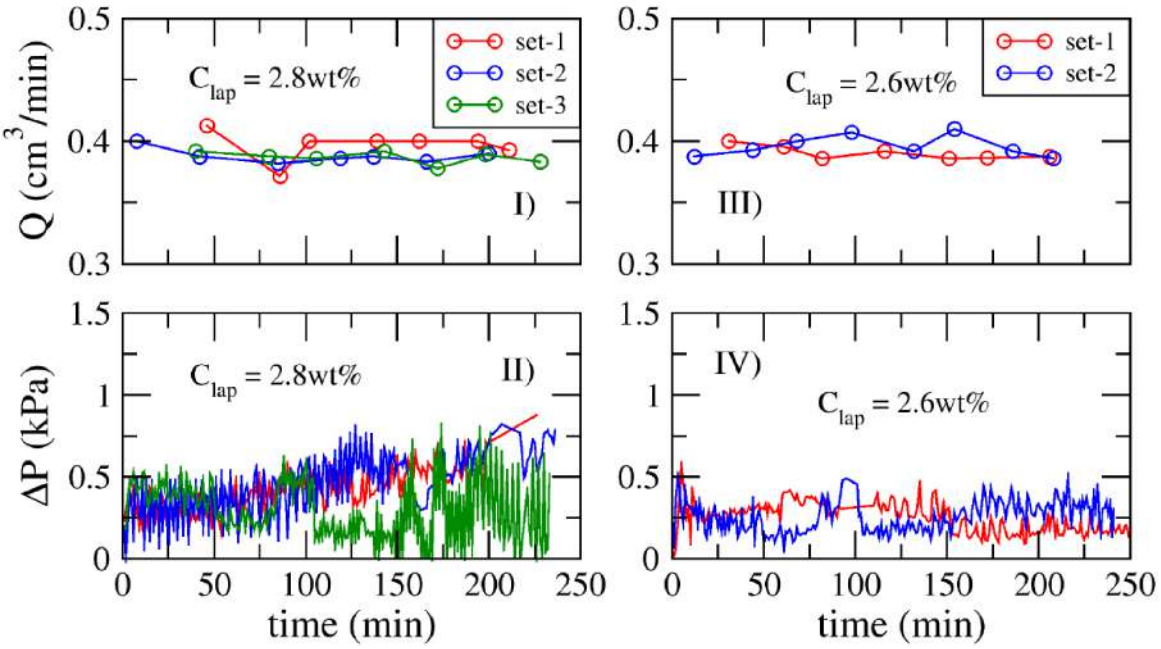

Figure 3.11 Flowrate vs time (I) and III)) and pressure drop vs time (II) and IV)) are measured for two different concentration of LAPONITE® (3mM) : 2.8wt% and 2.6wt%.

3.5 Pulsed flow system

All the experiments carried out in the continuous flow assembly described seemed to work reasonably well for moderate enough LAPONITE® (≤ 3 wt%) and salt concentration (≤ 6 mM). Any further increase in either of these values created homogenizing problems in the mixing vessel. The rapid ageing of LAPONITE® suspension at such high concentration led to formation of time varying non-uniform state of the suspension. Any increase in stirred speed was unable to eliminate this non-uniform state. A modification was, thus, proposed for the experimental system as described below.

3.5.1 Experimental system with salt solution pulse

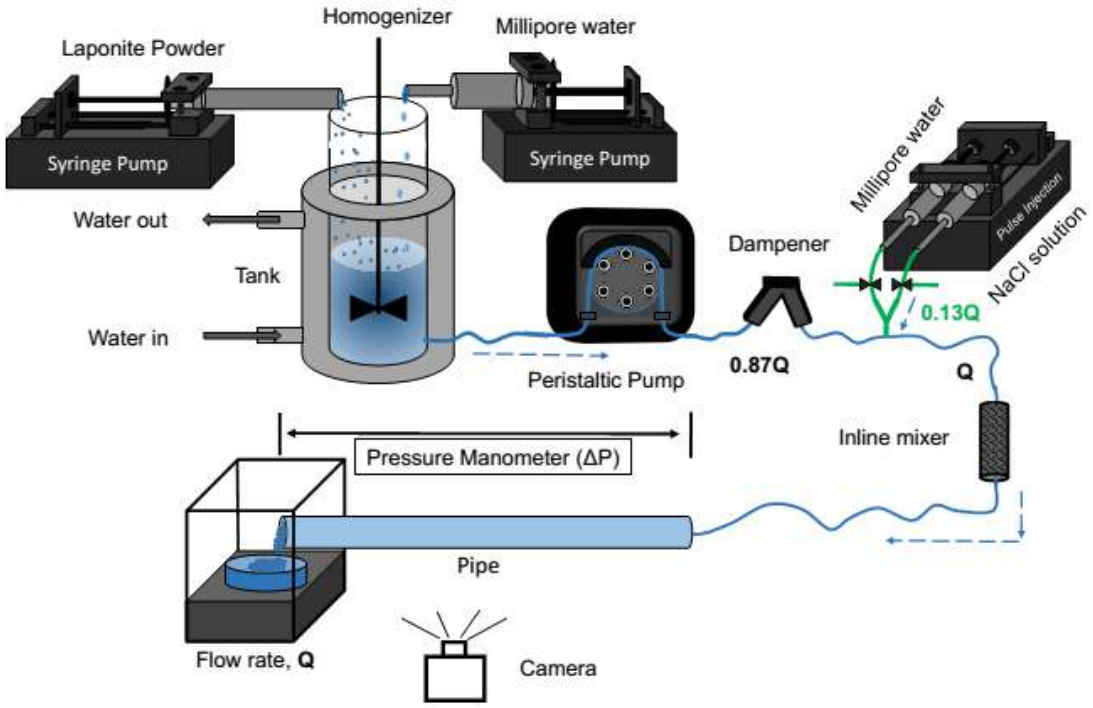

Figure 3.12 The experimental assembly showing continuous preparation of LAPONITE® suspension and continuous flow through a tube for the study of pulse triggered aging dynamics. The assembly allows alternate flow of water and aqueous salt in line for a fixed duration.

The modified experimental system is shown in fig. 3.12. In the modified experimental system and consequently methodology, only LAPONITE® suspension (3.1 wt%) was prepared in the mixing vessel. In the absence of any salt, the LAPONITE® suspension was not amenable to rapid ageing thereby allowing for a uniform state throughout. A second solution (salt solution or plain deionized water) was now introduced separately downstream of the dampener with a volumetric flow rate, $q_2 = 0.13q_1$, where q_1 is the outflow rate from the mixing vessel. The solution was introduced using a needle and then the two streams were mixed by passing them through a pinched tube static mixer (see section 3.5.2). The syringe pump that injects the second stream has two barrels so that it can flow either de-ionized water or a salt (NaCl) solution for a fixed duration. After mixing in the static mixer, the suspension is passed through the pipe. The advantages of this modification were manifold. First it allowed for a homogeneous state of the suspension in the mixing vessel.

Second, it mixed LAPONITE® with salt just before the pipe entry so that any possible changes arising in the suspension during the flow from mixing vessel to pipe were eliminated. This ensured a near constant state of suspension entering the pipe. Third, it allowed us to explore a wide range of salt concentrations, varied relatively easily and also for a fixed duration. However, these advantages depended on the relative mixing of the suspension and salt solution. This required an efficient mixer, the design and operation of which is described next.

3.5.2 Static mixer

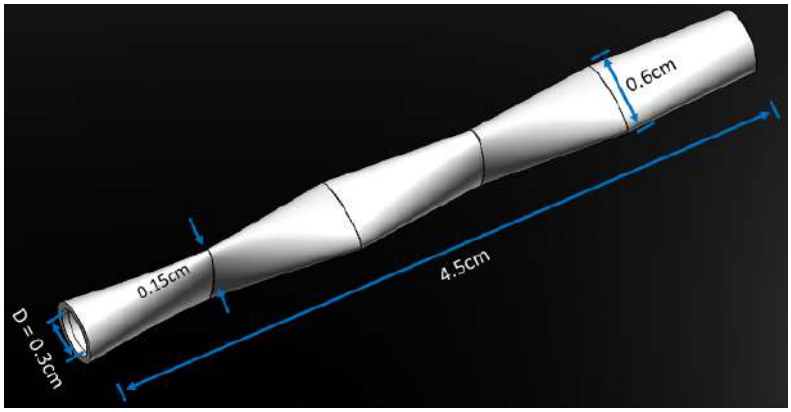

Figure 3.13 Drawing of static mixer for mixing of two streams.

The mixture of LAPONITE® suspension and salt solution is passed through an in-house static mixer before entering the pipe. The mixer comprised alternate stretched and compressed tube cross-section in flow direction. Inherent design of the mixer allows flow expansion and contraction subsequently leading to mixing. The schematic of the mixer is shown in fig. 3.13. This design has been analyzed in detail in the literature [95] and has been shown to offer efficient mixing by chaotic advection.

To verify the occurrence of mixing, a red dye is added in the pulsed stream of salt solution. Combined stream of dyed pulse stream and LAPONITE® suspension stream from mixing vessel was released to atmosphere through a transparent tubing of 0.3 cm diameter and 3 cm length. Without static mixer in line, dyed pulsed stream flows in streamline in (see fig. 3.14b). This indicates that both streams flow out without mixing. Then the designed mixer is placed inline before the transparent tubing and outflow of mixer is watched. The snapshot taken during the

outflow from the tubing is shown in fig. 3.14a. Uniform color along the tubing length and cross-section suggest reasonably good mixing for our study.

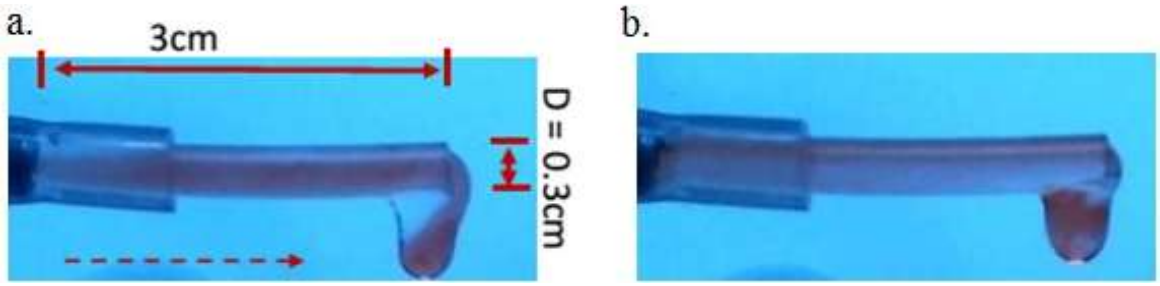

Figure 3.14 Digital image (snapshot) showing outflow of the mixture of LAPONITE® suspension and (red color) dyed salt solution taken in a transperent tube a. with presence of static mixer and b. without static mixer.

3.6 Concluding remarks

The experimental system is designed to investigate a complex, thixotropic fluid like LAPONITE® suspension. The methodology to use LAPONITE® suspension and salt streams separately provides ample opportunity to explore a wide range of thixotropic behavior. Moreover, it allows to focus on the exact effect of pipe flow and LAPONITE® ageing while eliminating any other peripheral issues that may influence the overall results. The continuous process methodology allows for experimenting over a significantly long duration while generating consistent results and preserving the state of suspension. The presence of suitably designed dampener and static mixer has improved the usability of the experimental system significantly. The final experimental system has been designed suitably, parameterized adequately which is capable to give results that are expected to elucidate the nuances and wealth of information within the relatively understudied flow characteristics of LAPONITE® suspensions.

Chapter - 4

4 Slip Behavior Of Pressure Driven Flow Of Laponite Suspension

4.1 Introduction

The velocity of liquid at the solid-liquid interface is commonly considered to be zero representing a non-slip boundary condition. Slip may, however, occur depending on liquid and solid properties. The non-wettability of the surface is one of the primary reasons for slip during the flow of Newtonian liquids [1-5]. During the laminar flow through a pipe, a distinct deviation from Poiseuille flow is observed due to slip, which is more pronounced for smaller system sizes [7]. Theoretically, it has been shown that the slip during pressure driven flows of Newtonian as well as viscoplastic fluids can be accounted in terms of effective slip length depending on system and material properties [8-10]. The predictions of velocity profiles based on scaling laws [9-10] seem to agree well with experimental measurements [11]. For shear-thinning visco-plastic fluids, wall slip was shown to be enhanced compared to that for Newtonian liquids, whereas in case of shear thickening fluids contrary effect was observed [56, 57].

All the studies mentioned above are carried out for time independent nature of fluid response. However, the time dependent or thixotropic fluids are encountered significantly in practice as described in Chapter 1 and 2 for which the slip behavior is poorly understood [17]. It has been shown that experimental measurements agree with theoretical scaling for the slip velocity expressed in terms of wall shear stress and slip length, even for time dependent material at steady state [44]. In recent experimental study, it was shown that the scaling law holds only when the material has yielded across the entire flowing cross section but not for co-existing solid-liquid regions or flows below the yield threshold [96].

In this chapter, we experimentally study the pressure driven flow of LAPONITE® suspension, a model thixotropic fluid, through a cylindrical tube to investigate the influence of slip on overall flow. The material properties, experimental system and the methodology remains the same as finalized toward the end of chapter 3. In the following we first briefly revise the experimental details for the benefit of the reader followed by observations and resulting discussion.

4.2 Experimental details

Dry LAPONITE® powder and deionized water (Millipore) were continuously added to a vessel and were subjected to high speed shearing (see fig. 3.12). The vessel was kept immersed in a water bath to maintain the temperature of LAPONITE®-water mixture at 25 °C throughout the experiments. The mixing vessel and mixing elements were coated with wax to avoid sticking LAPONITE® to the walls, that might result in variation in the dispersion concentration. The outflow rate (q_1) from the vessel, as set by the peristaltic pump was the same as the inlet flow rate to the vessel which was set by the syringe pump. This ensured that volume of suspension (V) in the vessel is maintained constant throughout. The average residence time of the material in the mixer is maintained at 45 min. The high shear mixing protocol ensured that the state of the LAPONITE® dispersion remained constant throughout the duration of the experiment. This was verified by measuring the outflow mass flow rate from the vessel which remained constant in time. To damp out fluctuations due to the peristaltic pump, the suspension is passed through a dampener. Downstream of the dampener, we introduce a second stream (volumetric flow rate, $q_2 = 0.13q_1$) using a needle and mix these streams by passing them through a pinched tube static mixer. The syringe pump that injects the second stream has two barrels so that it can flow either de-ionized water or a salt (NaCl) solution for a fixed duration. After mixing in the static mixer, the suspension is passed through the tube. The tube entrance has a uniformly diverging taper to minimize entrance effects due to the change in the cross-sectional area when the flow enters the tube. The tube exit is open to atmosphere, and we use a pressure gauge just before the tube entrance to measure the pressure drop across the tube length. The total volumetric flow rate ($Q = q_1 + q_2$) in the system is set by the peristaltic and syringe pumps. The measured outflow mass flow rate from the tube remained constant in time. Experiments are performed for three flow rates (Q = 0.46, 0.69, and 0.92 cm^3/min) and at three salt concentrations (6, 9 and 12 mM, after the two streams are mixed).

Tubes with different dimensions were used in the experiments: Glass tube (lengths 15.5 and 30 cm each with an internal diameter of 0.4 cm and 0.72 cm) and steel tube (length 23 and 53 cm each with an internal diameter of 0.1 cm). The LAPONITE® concentration in all experiments was kept unchanged throughout at 3.1 wt.%.

4.3 Flow visualization

To visualize the flow characteristics, a small amount of tracer particles (glass beads of diameter 50 microns obtained from Potters Inc.) were inserted in the flowing suspension just before the tube entrance for a small duration overlapping the salt solution pulse. The particles were observed to remain suspended in the flowing stream throughout the length of the tube given the high viscosity of the suspension. A green laser sheet (wavelength 532 nm and thickness 100 microns) was used to illuminate a planar section along the length of the tube of length 3 mm, located 3 cm upstream of the tube exit. The illuminated region in the tube was imaged at 10 frames per second using a digital camera placed orthogonal to the laser sheet plane. Only the upper half of the tube was imaged given the symmetric nature of the flow. However, it is to be noted that while the visualization system was good enough to qualitatively assess the nature of the flow, the image quality, unfortunately, was not good enough to quantitatively characterize the flow behavior accurately, the primary reason being significant scatter from the incident laser sheet.

4.4 Pressure drop measurements

The time variation of the pressure drop measured during the flow of LAPONITE® suspension (with or without added salt) is shown in fig. 4.1 for different pulsed durations. The measured pressure drop is the consequence of the resistance experienced by the flowing suspension pumped at a constant rate of 0.46 cm^3 /min. The pressure drop for the LAPONITE® suspension without salt (shown as red solid line in the fig. 4.1) is quite negligible and remains constant throughout at 0.05 kPa. We refer to this value as the base or reference pressure drop. The LAPONITE® suspension, in this case, behaves like a liquid as observed from the outflow from the tube. It is expected that the presence of salt concentration in the LAPONITE® suspension will cause it to age rapidly with an evolving microstructure comprising sample spanning aggregates, thereby increasing the overall

viscosity. This increase in viscosity leads to increased pressure difference above the base value. As seen from fig. 4.1, the pressure drop reaches an increasing highest value with increasing salt pulse duration (defined as Δt_p) while following the same path all along. The near saturation state is reached for Δt_p = 80 mins suggesting a balance in the microstructure of the LAPONITE® suspension between salt induced ageing and flow effects. Duration of pulses smaller than 80 mins do not seem to be enough to cause saturation in the pressure drop value. We consider data for the pulsed duration of 80 mins for all the analysis in the remainder of this chapter.

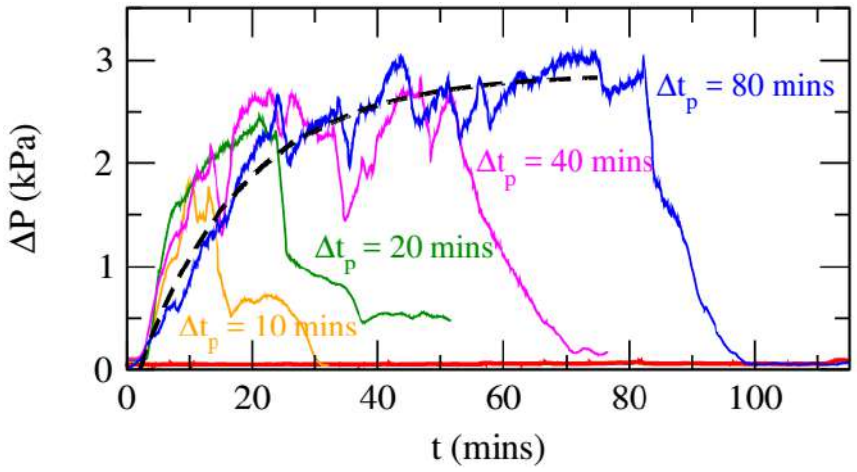

Figure 4.1 time Time (t) dependent pressure drop (ΔP) for the flow of LAPONITE® suspension at a constant rate (Q = 0.46 cm^3 /min) through the tube of length (L = 15.5 cm) and diameter (D = 7.2 mm) for a fixed salt concentration (C_s = 9mM). Red solid line represents data without addition of salt, while other colored lines represent data for addition of salt solution in pulses of different times as specified in the figure. The black dashed line represents a fitted non-linear equation to the data for Δtp = 80 mins to extract the saturated pressure drop (ΔP_s) value. See text for more details.

Following the stoppage of the pulse after Δt_p, the pressure returns to the base value after a brief time period. This indicates that the subsequent flow of Laponite suspension, bereft of salt, requires that much time to remove the salt completely from the pipe. It can be noted that the timescales leading to the saturated value of pressure drop and while reverting to the base value are not the same. We believe that this difference owes its origin to the significant heterogeneity in the microstructures formed within the system, the time for removal of which need not be the same as

that for their formation. The pressure drop variation is not smooth throughout but shows oscillations about the fitted curve. These oscillations may be attributed to a stick-slip kind of behavior, possibly caused due to local changes in the microstructure due to flow. However, the details of these microstructural changes cannot be captured using the experimental tools used in this work. Thus, it is difficult to elaborate on the origin of the forces responsible for such behavior. Similar qualitative behavior for pressure drop variation is also observed for different tube diameters, lengths, salt concentration, and flow rates investigated in this work (refer fig. 4.2). The following representative experimental data suggests that steady pressure drop per unit length decreases with flow rate, pipe diameter and with decreasing salt concentration.

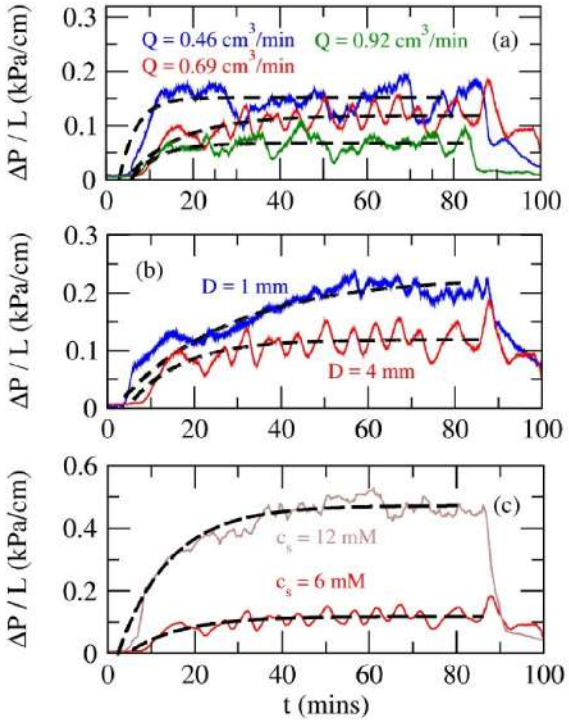

Figure 4.2 Pressure drop across the pipe per unit length with time (t) is plotted for 80 minutes salt pulse duration showing the behaviour at different (a) flow rates (keeping fix C_s= 6 mM and pipe dimensions, D = 4 mm and L =15.5 cm), (b) pipe diameters (keeping fix C_s = 6 mM and Q = 0.69 cm^3/min) and (c) salt concentrations (keeping fix Q = 0.69 cm^3/min and pipe dimensions, D = 4 mm and L = 15.5 cm). The black dashed line represents a fitted non-linear equation to the data.

The value of the plateau or the saturated pressure drop ($\Delta P_s/L$) is extracted by fitting the data for the 80 minutes salt solution pulse with an exponential expression of the form $\Delta P/L = C_1(1 - \exp(-t/\tau)) + C_2$. The saturation pressure drop (ΔP_s) is then obtained as $C_1 + C_2$ at large enough value of time (t). The fit of this equation (black dashed line) is shown in fig. 4.1 as well as in fig. 4.2. The parameters C_1 , C_2 and τ were simply used to fit the expression to the data. No specific behavior was, however, found for all the three parameters. The pressure drop values presented in subsequent sections have been acquired during the flow of Laponite suspension pre-mixed with salt solution, pulsed for a duration (Δt_p) of 80 minutes. We, next, study the effect of different experimental variables on saturated pressure drop. For each case, 2 or 3 independent runs were performed, and the average data are reported for all the cases.

4.5 Result and discussion

In the following sections we have discussed the effect of tube length, flow rate, tube diameter and salt concentration on the saturated value of pressure drop (ΔP_s). We, then, try and show the scaling of all the data based on heuristic arguments.

4.5.1 Effect of tube length on saturated pressure

The variation of ΔP_s and ΔP_s/L with flow rate (Q) for two different tube lengths at fixed tube diameter (D = 0.1 cm) and salt concentration (C_s = 9 mM) shown in fig. 4.3. For a given flow rate, the pressure drop increases with the increase in tube length. However, the pressure drop per unit length (ΔP_s/L) is nearly independent of the tube length as shown in fig 4.3(b). This suggests that the observed behavior and underlying mechanism are not localized, but it remains the same everywhere along the tube length.

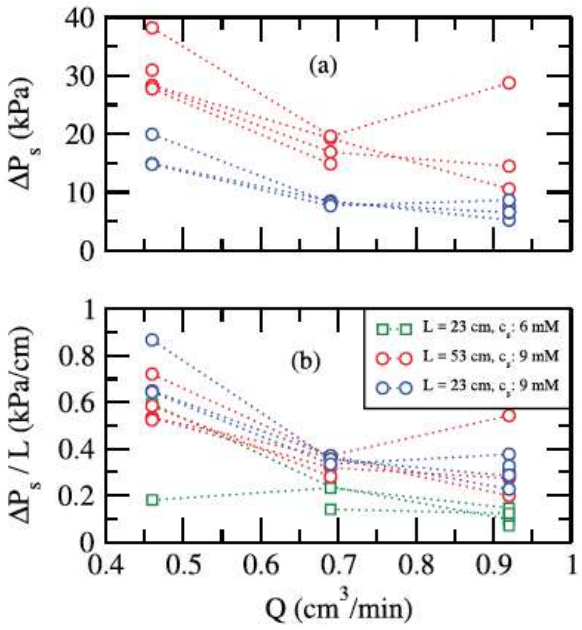

Figure 4.3 Variation of (a) saturated pressure drop (ΔP_s) with flow rate in a tube of diameter (D = 0.1 cm) and salt concentration (C_s = 9 mM) for two different tube lengths and (b) Variation of $\Delta P_s/L$ with flow rate in a tube of diameter (D = 0.1 cm) and two salt concentrations and tube lengths.

Interestingly, the data in fig. 4.3(b) show that the saturated pressure drops decreases monotonically with increase in the flow rate. Furthermore, this decrease in the pressure drop is more prominent at higher salt concentration. At much higher salt concentration (C_s = 12 mM), a rapid increase in viscosity led to intermittent flow causing problems in pressure drop measurements. This behavior of pressure drop is qualitatively opposite to that predicted by the Poiseuille equation. To rationalize this, we consider the possibility that higher shear rates at higher Q might result in a flow-induced breakdown of aggregated network LAPONITE® particles microstructure in the bulk of the suspension. This microstructural change correlates with a decrease in viscosity and therefore a decrease in ($\Delta P_s/L$) with increase in Q. Such a behavior, akin to a shear thinning fluid, will always yield an increase in the steady (or saturated) state pressure drop with an increase in the flow rate in contrast to the observed behavior over here. Further, we anticipate that such flow induced microstructural breakage will occur locally—thus, an increase in tube length should result in greater microstructural change and lower. In this situation, ($\Delta P_s/L$)

will not be independent of the tube length, which is inconsistent with the behavior observed in fig. 4.3(b). Therefore, the decrease in ($\Delta P_s/L$) with Q is not a consequence of flow induced changes in LAPONITE® microstructure in the bulk of the tube. We now consider the possibility that slip of LAPONITE® suspensions at the tube walls reduces the pressure drop. Similar behavior, i.e., increase in the flow rate under constant pressure gradient, been observed previously for pressure-driven flow of Newtonian liquids [7] and visco-plastic fluids [11]

4.5.2 Effect of tube diameter and salt concentration on saturated pressure

Figure 4.4 shows the variation of $\Delta P_s/L$ with tube diameter for three different flow rates and three different salt concentrations. The values of $\Delta P_s/L$ decrease with increase in tube diameter at all flow rates and salt concentrations employed. This effect is more pronounced at smaller tube diameters. The inverse dependence is in line with the behavior expected during the Poiseuille flow, i.e. smaller the cross-sectional area available for flow, higher is the pressure drop needed to achieve the same flow rate. Second, the magnitude of saturated pressure drop increases significantly with increase in salt concentration. Now, increase in salt concentration significantly accelerates ageing of LAPONITE® suspensions, thereby increasing its effective viscosity [76]. Naturally, the pressure drop required to pump the fluid at a constant rate is expected to increase with increase in the effective viscosity, again in line with that expected from the Poiseuille flow. The effective viscosity rises rapidly with salt concentration, so that pressure drop measurements could be obtained only at the highest flow rate employed for experiments using the smallest tube diameter (D = 0.1 cm) at the highest salt concentration employed (C_s = 12 mM).

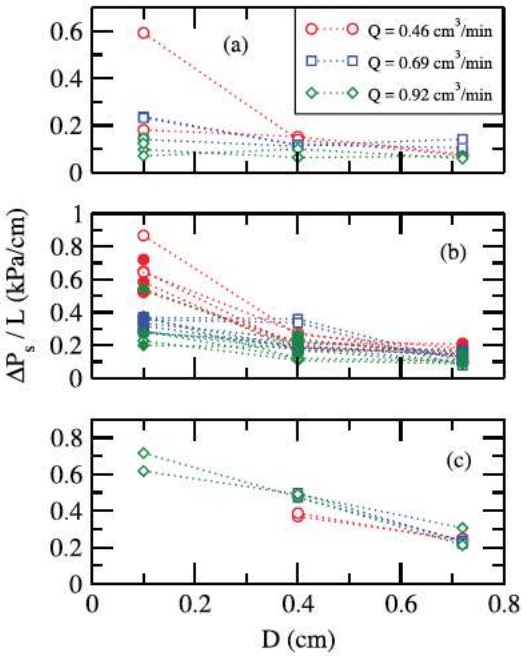

Figure 4.4 (a) Variation of saturated pressure drop per unit length ($\Delta P_s/L$) with tube diameter (D) for three flow rates (Q). Panels (a), (b) and (c) represent, respectively, data obtained for salt concentrations, C_s = 6 mM, C_s = 9 mM and C_s = 12 mM. Open circles represent data for L = 23 cm, filled circles represent data for L = 53 cm, open squares and diamonds represent data for L = 15.5 cm and filed squares and diamonds represent data for L = 30 cm.

The parametric dependence described above shows distinct dependence of the measured pressure drop on three variables, namely flow rate, tube diameter and salt concentration. The salt content tends to influence the suspension aging dynamics while flow-induced structure breackage is governed by shear rate which is closely related the tube diameter and flow rate. However, both these effects seem to occur on the backdrop of flow slippage as evidenced by the observed dependence on employed flow rate. This encourages us to seek a non-linear dependence, akin to a scaling law relating these three variables with the saturated pressure drop. In the next section, we attempt to derive the scaling relation taking into account the experimental observations.

4.6 Scaling behavior

The LAPONITE® suspension exhibits significant thixotropy, i.e., its state evolves continuously with waiting time. A steady state is, thus, not achievable in such a system, thereby precluding the existence of a stress constitutive equation comprising a steady shear viscosity. However, the experimental observations exhibit a steady (or saturated) state pressure drop following the initial transient period (see fig. 4.2). Given our primary interest in understanding the behavior of steady pressure drop, we assume a unidirectional, steady state flow of LAPONITE® suspension through the tube. The axial component of the Navier-Stokes equation for the pressure driven flow through a horizontal cylindrical pipe, then, is simplified to

$$\frac{1}{r}\frac{d(r\tau_{rz})}{dr} = \frac{\Delta P_s}{L} \tag{4.1}$$

Where, r is the radial coordinate and z is the axial coordinate. ΔP_s is a steady state pressure drop across the pipe length (L) and τ_{rz} is the local shear stress. Integrating eq. 4.1 leads to

$$r\tau_{rz} = \frac{\Delta P_s}{L}\frac{r^2}{2} + C_1 \tag{4.2}$$

where, the constant of integration (C_1) evaluates to zero considering that shear stress is zero at the along the pipe axis (i.e. r = 0) and the shear stress is now written as

$$\tau_{rz} = \frac{\Delta P_s}{L}\frac{r}{2} \tag{4.3}$$

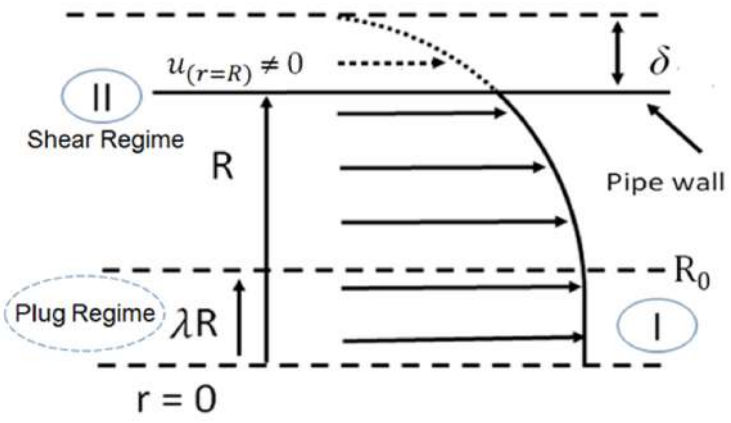

Figure 4.5 Velocity distribution with slip at pipe wall during flow of Bingham fluid in a pipe. Plug regime indicates zero velocity gradient and shear regime shows Newtonian fluid flow behaviour. δ is slip length.

Typically, LAPONITE® suspension exhibits a yield stress (τ_y) and a shear flow post yielding. To simplify the representation of the observed behavior, we consider Bingham fluid like behavior for which the shear stress (τ_{rz}) is expressed as

$$\tau_{rz} = \tau_y - \mu \frac{du}{dr} \tag{4.4}$$

The above stress constitutive equation represents a fluid which behaves like a (i) solid for applied shear stress lesser than the yield stress (τ_y) and (ii) Newtonian liquid for applied stress larger than the yield stress. A typical pipe flow with yielding in a finite region near the wall is represented by a plug profile in the central region and a shear profile near the wall (see fig. 4.5). Inserting eq. 4.4 in eq. 4.3 results in

$$\frac{du}{dr} = -\frac{\Delta P_s}{L}\frac{r}{2\mu} + \frac{\tau_y}{\mu} \tag{4.5}$$

Now considering that the velocity gradient (du/dr) is zero at the boundary ($r = \lambda R = R_0$) between the central plug region and external shear region results in

$$R = \tau_y \left(\frac{2L}{\Delta P_s}\right) \tag{4.6}$$

which after substituting in eq. 4.5 and integrating gives following expression for axial velocity (u) profile

$$u = -\frac{\Delta P_s}{L}\frac{1}{2\mu}\left(\frac{r^2}{2} - \lambda R r\right) + C_2 \tag{4.7}$$

where, C_2 is the constant of integration obtained by considering the slip velocity at the boundary. The schematic of the slip, plug and shear velocity profile is shown in fig. 4.5 for ease in understanding the underlying phenomena.

Here we assume slip phenomenon to explain observed inverse dependence of ΔP on Q. When slip occurs, fluid at pipe wall has a non-zero velocity. In reference to slip, δ is slip length from pipe wall to a point where no boundary condition exists. Using these boundary conditions at the wall to account for slip (at r = R, u = u (r = R) and at r = (R + δ), u = 0) results in following two expressions for the velocity.

$$u = -\frac{\Delta P_s}{L}\frac{R^2}{4\mu}\left(\frac{r^2 - (R+\delta)^2}{R^2} - \frac{2\lambda(r - R - \delta)}{R}\right) \tag{4.8}$$

$$u(r = R) = \frac{\Delta P_s}{L}\frac{R^2}{4\mu}\left(\left(1 + \frac{\delta}{R}\right)^2 - 2\lambda\left(\frac{\delta}{R}\right) - 1\right) \tag{4.9}$$

Given that the flow is axisymmetric, the volumetric flow in pipe is given by,

$$Q = 2\pi\left(\int_0^{\lambda R} u(r)\, r dr + \int_{\lambda R}^{R} u(r)\, r dr\right) \tag{4.10}$$

Substituting the velocity expression from 4.8, the volumetric flow rate is given as

$$= \frac{\pi D^4}{64}\left(\frac{\Delta P_s}{\mu L}\right)\left(1-\lambda+\frac{2\delta}{D}\right)^2\left[1-2\left(\frac{(1-\lambda)^2}{4}+\frac{(1-\lambda)}{3}\lambda\right)\right] \quad (4.11)$$

where, $\lambda = \tau_y/(\Delta P_s D/4L)$ and δ is the slip length. The overall form of the eq. 4.11 is consistent with that obtained previously for a visco-plastic fluid [52].

The value of $(\Delta P_s D/4L)$, i.e. the wall shear stress, as measured from the experiments is of order [O(10 Pa)], similar to the yield stress values of LAPONITE® dispersions of comparable concentration and ionic strength as shown in table 4-1 below. This implies that the material does not shear anywhere in radial direction and it flows like a solid plug inside the pipe, viz. $\lambda \to 1$. This is clearly seen through flow visualization as described in earlier section. The material yielding is then the primary reason for slip in present system which is consistent with previous reports [96]. Based on these arguments, we consider slip as the predominant behavior which, thereby, leads to simplification of equation (4.11) as

$$Q = \frac{\pi}{16}\left(\frac{\Delta P_s}{L}\right)\frac{D^2\delta^2}{\mu} \quad (4.12)$$

In above equation, all quantities except δ, are either known, measured, or can be estimated. We infer the behavior of δ based on our experiments. Using a linear dependence i.e., $\delta \propto Q$ in eq. (4.12), we observe that the experimentally obtained inverse relation between ΔP_s and Q is recovered. We reiterate that the linear dependence of δ on Q is invoked to rationalize the data and is not based on any reasoning from the literature. We do note, however, that experiments by Zhu and Granick [50] for Newtonian liquids do show that slip length increases with shear rate. Similar interpretation is also supported by Aktas' experiments [44]. Furthermore, neither can the dependence of slip length on system size be obtained from literature [46, 54, 97]. We, thus, consider $\delta \propto Q/f(D)$, where the exact functional dependence on tube diameter is obtained from a fit to the experimental data.

Table 4-1 Yield stress values (τ_y) of LAPONITE® suspension reported in literature for our experimental flow system ($C_{laponite}$ = 3.1wt%, NaCl C_s = 6 - 12 mM).

Reference	$C_{laponite}$	Salt	C_s (mM)	τ_y (Pa)
Pek-Ing. A., et al. [98]	3 wt%	KNO_3	5 - 20	40 - 110
Lin, Y., et al. [90]	3.5 wt%	-	-	45
Ranganathan, V., et al., [99]	3 % wt/volume	NaCl	0.5	6

Finally, the extensive literature on the effect of ionic strength on LAPONITE® ageing indicates that the dependence on salt concentration is highly nonlinear [76, 100, 101]. Again out of convenience we invoke a non-linear relation where the viscosity varies as power law with respect to the salt concentration, i.e. $\mu \propto C_s^n$. We note here that the effective viscosity (ratio of shear stress to shear rate) will tend to infinity as evidenced from eq. 4.4. However, the flow rate in plug regime will be governed by the value of μ with the above mentioned dependence on salt concentration. Using these assumptions, eq. 4.12 can be expressed as

$$\frac{\Delta P_s}{L} \propto \frac{C_s^n}{Q\,D^2}\,[f(D)]^2 \qquad (4.13)$$

Table 4-2: Fitting parameters of master curve using equation (4.13) for experimental data and respective δ vs D fitting is given bellow.

Exponent of C_s (n)	2.5	2.2	2	1.8	1.5
R^2 (Collapse of experimental data on a master curve)	0.738	0.735	0.7306	0.7234	0.706
Exponent (m) for $f(D) \propto D^m$	0.63	0.66	0.68	0.70	0.72
R^2 (fit for $f(D) \propto D^m$)	0.9885	0.9909	0.9921	0.9932	0.9943

The experimental results for all flow rates, tube diameters and salt concentrations studied are shown in the main panels of fig 4.6 for three different values of exponent "n". For each case, we

adjust f (D) so as to collapse the data on a universal curve by shifting individual data sets. We observe that $[f(D)]^2$ shows a power-law dependence on tube diameter (D) with slightly different exponents as shown in insets of fig. 4.6. As seen from the figure and accompanying table 4-2, the accuracy of the fit and the collapse is similar for a range of values of exponents (n). The precise value of the exponent will, however, require additional experiments and theoretical considerations beyond the scope of this work. However, the collapse of data from experiments carried over a wide range of parameters on a master curve is remarkable given the complexity of microstructure formation in thixotropic LAPONITE® suspensions and simultaneously occurring number of phenomena. From the fit to the experimental data, and considering n = 2, we obtain the final relation as

$$\frac{\Delta P_s}{L} \propto \frac{C_s^2}{Q\, D^{0.6\ 4}} \tag{4.14}$$

Further, our data suggest an empirical correlation for the slip length, given as $\delta \propto QD^{-0.6\ 8}$. Though not identical to our experimental system, we note that the slip length has been theoretically shown to scale as D^{-1} for the flow of water through nanopores [54].

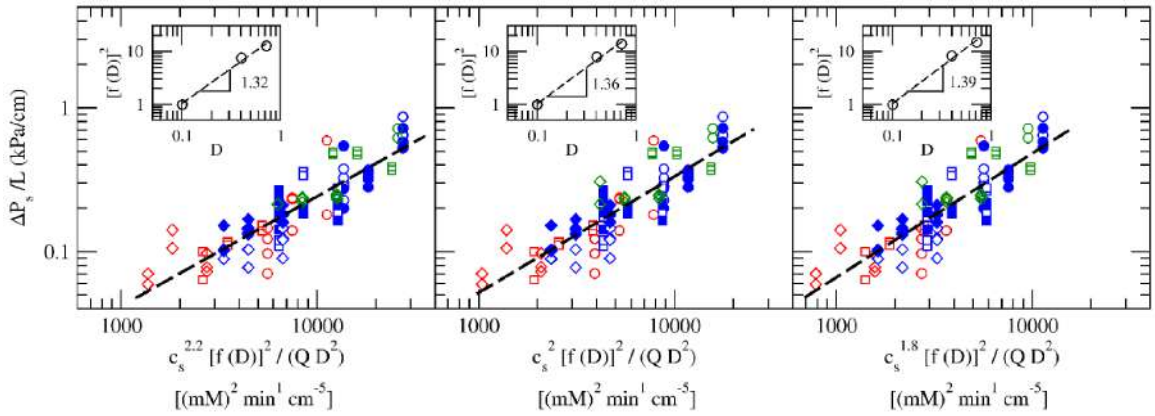

Figure 4.6 Fit of saturated pressure drop per unit length ($\Delta P_s/L$) with different experimental parameters investigated for (i) $C_s^{2.2}$, (ii) C_s^2 and (iii) $C_s^{1.8}$. Each data point shows individual experiment data. Different color represents salt variations. Various symbols represent diameter variations. Open and closed symbol indicate different pipe lengths. Inset: Variation of shift factor $[f(D)]^2$ with tube diameter.

4.7 Conclusion

In summary, we have investigated the slip behavior for pressure driven flow of a thixotropic material through a cylindrical tube. While the LAPONITE® suspension is thixotropic, we obtain steady state flow behavior over a range of experimental conditions. The steady state is envisaged as a balance between the inherent structure formation of LAPONITE® and possible breakage due to flow. The steady state is represented by near time independent (or saturated) pressure values measured during the flow of suspension through the tube.

Remarkably, the saturated pressure drop shows an inverse relation with the flow rate, in contrast to our expectation based on the Poiseuille relation. These observations can be rationalized by invoking slip of LAPONITE® suspensions at the tube walls. We show that the observed experimental results can be accounted for if a linear dependence is assumed between the slip length and flow rate and the material can be described using a Bingham constitutive equation. The observed scaling behavior indicates that the slip length varies linearly with the flow rate and inversely with the tube diameter.

It is to be, however, noted that the scaling behavior is obtained purely based on a fit to the data. The assumed variations of the key variables cannot be obtained from the literature, and their deduction through independent measurements is not within the scope of this work. The reasonably good scaling behavior suggests that these adhoc assumptions are not without merit. The remarkably simple dependence of the flow behavior of a complex thixotropic material should pave the way for a more involved theoretical treatment of flowing thixotropic materials.

Chapter - 5

5 Conclusions And Future Work

Pressure driven flows of thixotropic (time dependent ageing) materials through pipes or capillaries are encountered in many industrial operations. Such systems are notorious for flow blocking due to agglomeration tendency of the flowing material thereby forming a sample spanning microstructure. We have studied the flow of a model thixotropic material (LAPONITE® suspension) through pipes under constant flow rate conditions. The objective was to correlate the material properties, rheology and flow properties and obtain a deeper understanding of pipe flow behavior. LAPONITE® suspension was chosen as model material due to abundant literature available characterizing its rheology and microstructural behavior.

Experiments were performed in a continuous manner with steady inflow of LAPONITE® and water in a tank from where it was pumped to a pipe section using peristaltic pump. The continuous arrangement was required to offset the ageing tendency of LAPONITE® suspension in tank and allowing for a constant state of material entering the pipe. The ageing tendency and its effect on the flow was captured by inserting a pulsed stream of salt into the flowing LAPONITE® suspension just before the pipe entry. Experiments were performed for various tube diameters, tube lengths, flow rates, salt concentration and fixed LAPONITE® concentration. A robust experimental system was developed over several trials while accounting for various flow behaviors and included novel elements like pulsating dampeners and flow mixers. The flow behavior of LAPONITE® suspension was ascertained by measuring the pressure drop across the pipe length. Qualitative information about the flow was also obtained using laser fluorescence and camera imaging along a pre-defined cross-section of the pipe. The pressure variation exhibited a time increase followed by a saturated value at long times as long as the salt solution was streamed into

the flow. The pressure-time curves were fitted with an exponential function to obtain the saturated pressure for various system variables.

The saturated pressure drop per unit length exhibited a decrease with increasing flow rates unlike typically observed for a Poiseuille flow. The behavior was independent of tube lengths investigated. Further, the pressure drop showed a decrease with increasing particle diameter and a substantial increase with increase in salt concentration. The second and third observation, respectively, indicate lesser cross-section available for flow and higher ageing tendency. The non-intuitive pressure drop vs flow rate behavior, however, suggested possibility of the occurrence of slippage of the flow at the pipe walls.

Assuming the material to behave like a Bingham (yield stress) fluid and a laminar unidirectional flow, the momentum balance equation was solved to an expression for pressure drop relating with flow rate, pipe diameter and fluid viscosity. The slip was accounted by following the methodology presented in the literature. The wall slip occurrence was attributed to material yielding resulting in plug like flow across the pipe cross section as verified through tracer particles and laser fluorescence imaging. Assuming a non-linear flow rate dependence of slip length and salt concentration dependence of viscosity, a non-linear scaling relation was obtained for the entire data spanning various salt concentrations, flow rates and pipe diameter and lengths. The scaling relation also suggested a linear dependence of slip length with flow rate and an inverse dependence with pipe diameter.

The scaling relation was, however, purely based on a fit to the data. Some of the assumed variations could not be ascertained from literature and will require further studies. The reasonably good scaling behavior suggests that the adhoc assumptions are not without merit. Moreover, the scaling relation can be considered as a first step towards a comprehensive understanding of the flow of thixotropic materials through pipes and can act as a foundation for a more involved theoretical treatment in future.

Clearly much more work remains to be done in this very interesting flow problem and below we suggest a few ideas that can be pursued in future.

- Exploration of the behavior for extreme circumstances whereby a complete blocking of the flow is observed and correlate with material properties and operating conditions. Herein

the transition from slip to blocking behavior will be an interesting aspect to study. Consider the use of constant pressure conditions if constant flow rate conditions preclude observing complete blockage.

- Carry out a thorough and detailed visualization to understand the localized flow and its relation with localized blockage and overall flow. This can be complemented with rheology experiments to connect with possible microstructure understanding.
- Further explore the range of pipe dimensions, flow rates and salt concentrations to adequately understand the applicability of obtained scaling relation. Study of different model materials, having different rheology-microstructure relations to ascertain the flow behavior. These studies will allow for a much more robust, though complicated scaling relation with a much expanded envelope across a larger variable range.
- Extend the work to study the flow of crude oil or relevant practical material through longer flow loops, varying temperatures and varying flow rates. The results would be of utmost importance to industries handling these materials on a routine basis. A correlation accounting for the additional variables will be quite desirable in practical systems.

References

1. Irgens, F., *Rheology and Non-Newtonian Fluids*. 2013: Springer.
2. Chhabra, R.P. and Richardson, J.F., *Non-Newtonian Flow and Applied Rheology: Engineering Applications*. 2011: Elsevier Science.
3. Chilton, R.A. and Stainsby, R., *Pressure loss equations for laminar and turbulent non-Newtonian pipe flow.* Journal of hydraulic engineering, 1998. **124**(5): p. 522-529.
4. Bobok, E., *Fluid mechanics for petroleum engineers*. 1993: Elsevier.
5. Deshpande, A.P. and Sunil Kumar, P.B., *Rheology of Complex Fluids*. 2010: Springer.
6. Krieger, I.M. and Dougherty, T.J., *A mechanism for non-Newtonian flow in suspensions of rigid spheres.* Transactions of the Society of Rheology, 1959. **3**(1): p. 137-152.
7. Batchelor, G., *The effect of Brownian motion on the bulk stress in a suspension of spherical particles.* Journal of fluid mechanics, 1977. **83**(1): p. 97-117.
8. Maranzano, B.J. and Wagner, N.J., *The effects of interparticle interactions and particle size on reversible shear thickening: Hard-sphere colloidal dispersions.* Journal of Rheology, 2001. **45**(5): p. 1205-1222.
9. Schnell, E., *Slippage of water over nonwettable surfaces.* Journal of Applied Physics, 1956. **27**(10): p. 1149-1152.
10. Choi, C.-H., Westin, K.J.A., and Breuer, K.S., *Apparent slip flows in hydrophilic and hydrophobic microchannels.* Physics of fluids, 2003. **15**(10): p. 2897-2902.
11. Betts, J.G., *Anatomy and physiology*. 2013: OpenStax College, Rice University.
12. Hammer, G.D. and McPhee, S.J., *Pathophysiology of disease: An Introduction to Clinical Medicine 7/E*. 2014: McGraw-Hill Education.
13. Bignold, L.P., *Principles of tumors*. 2015: Elsevier, Mica Haley.
14. Donelli, G., Guaglianone, E., Di Rosa, R., Fiocca, F., and Basoli, A., *Plastic biliary stent occlusion: factors involved and possible preventive approaches.* Clinical Medicine & Research, 2007. **5**(1): p. 53-60.
15. *HEARTS: Technical package for cardiovascular disease management in primary health care*. 2016, World health organization
16. King, M.W., Bambharoliya, T., Ramakrishna, H., and Zhang, F., *Coronary Artery Disease and The Evolution of Angioplasty Devices.* Springer, 2020.
17. Johnson, W., Onuma, O., Owolabi, M., and Sachdev, S., *Stroke: a global response is needed.* Bull World Health Organ, 2016. **94**: p. 634–634A.
18. Cronenwett, J., Murphy, T., Zelenock, G., Whitehouse Jr, W., Lindenauer, S., Graham, L., Quint, L., Silver, T., and Stanley, J., *Actuarial analysis of variables associated with rupture of small abdominal aortic aneurysms.* Surgery, 1985. **98**(3): p. 472-483.
19. Fillinger, M.F., Raghavan, M.L., Marra, S.P., Cronenwett, J.L., and Kennedy, F.E., *In vivo analysis of mechanical wall stress and abdominal aortic aneurysm rupture risk.* Journal of vascular surgery, 2002. **36**(3): p. 589-597.
20. Costamagna, G., Bulajic, M., Tringali, A., Pandolfi, M., Gabbrielli, A., Spada, C., Petruzziello, L., Familiari, P., and Mutingnani, M., *Multiple stenting of refractory pancreatic duct strictures in severe chronic pancreatitis: long-term results.* Endoscopy, 2006. **38**: p. 254-259.
21. Gupta, R. and Reddy, D.N., *Stent selection for both biliary and pancreatic strictures caused by chronic pancreatitis: multiple plastic stents or metallic stents?* Journal of Hepatobiliary Pancreatic Sciences, 2011. **18**: p. 636-639.
22. Valenti, R., Vergara, R., Migliorini, A., Parodi, G., Carrabba, N., Cerisano, G., Dovellini, E.V., and Antoniucci, D., *Predictors of reocclusion after successful drug-eluting stent–supported*

percutaneous coronary intervention of chronic total occlusion. Journal of the American College of Cardiology, 2013. **61**(5): p. 545-550.
23. TND. *stroke*. Available from: https://www.topneurodocs.com/stroke/.
24. UCSF. *Heart Disease*. Available from: http://www.healthyheart.ucsf.edu/heartdisease-facts.shtml.
25. Theyab, M. and Yahya, S., *Introduction to wax deposition.* Int J Petrochem Res, 2018. **2**(1): p. 126-131.
26. Xie, Y., Chen, D., and Mai, F., *Economic pigging cycles for low-throughput pipelines.* Advances in Mechanical Engineering, 2018. **10**(11): p. 1687814018811198.
27. Wang, W., Huang, Q., Li, S., Wang, C., and Wang, X. *Identifying optimal pigging frequency for oil pipelines subject to non-uniform wax deposition distribution*. in *International Pipeline Conference*. 2014. American Society of Mechanical Engineers.
28. Corvisier, P., Nouar, C., Devienne, R., and Lebouché, M., *Development of a thixotropic fluid flow in a pipe.* Experiments in fluids, 2001. **31**(5): p. 579-587.
29. Oh, S., Song, Y.-q., Garagash, D.I., Lecampion, B., and Desroches, J., *Pressure-driven suspension flow near jamming.* Physical Review Letters, 2015. **114**(8): p. 088301.
30. O'Donnell, H. and Butler, F., *Time-dependent viscosity of stirred yogurt. Part II: tube flow.* Journal of Food Engineering, 2002. **51**(3): p. 255-261.
31. Cunha, J.P., de Souza Mendes, P.R., and Siqueira, I.R., *Pressure-driven flows of a thixotropic viscoplastic material: Performance of a novel fluidity-based constitutive model.* Physics of Fluids, 2020. **32**: p. 123104.
32. de Souza Mendes, P.R., Abedi, B., and Thompson, R.L., *Constructing a thixotropy model from rheological experiments.* J. Non-Newtonian Fluid Mechanics, 2018. **261**: p. 1-8.
33. Zarraga, I.E., Hill, D.A., and Leighton Jr, D.T., *The characterization of the total stress of concentrated suspensions of noncolloidal spheres in Newtonian fluids.* Journal of Rheology, 2000. **44**(2): p. 185-220.
34. Leighton, D. and Acrivos, A., *The shear-induced migration of particles in concentrated suspensions.* Journal of Fluid Mechanics, 1987. **181**: p. 415-439.
35. Hampton, R., Mammoli, A., Graham, A., Tetlow, N., and Altobelli, S., *Migration of particles undergoing pressure-driven flow in a circular conduit.* Journal of Rheology, 1997. **41**(3): p. 621-640.
36. Lyon, M. and Leal, L., *An experimental study of the motion of concentrated suspensions in two-dimensional channel flow. Part 1. Monodisperse systems.* Journal of fluid mechanics, 1998. **363**: p. 25-56.
37. Churaev, N., Sobolev, V., and Somov, A., *Slippage of liquids over lyophobic solid surfaces.* Journal of Colloid & Interface Science, 1984. **97**(2): p. 574-581.
38. BLARE, T.D., *Slip Between a Liquid and a Solid: D.M. Tolstoi's (1952) Theory Reconsidered.* Colloids and Surfaces, 1990. **47**: p. 135-145
39. Neto, C., Evans, D.R., Bonaccurso, E., Butt, H.-J., and Craig, V.S., *Boundary slip in Newtonian liquids: a review of experimental studies.* Reports on progress in physics, 2005. **68**(12): p. 2859.
40. Bonaccurso, E., Butt, H.-J., and Craig, V.S., *Surface roughness and hydrodynamic boundary slip of a Newtonian fluid in a completely wetting system.* Physical review letters, 2003. **90**(14): p. 144501.
41. Boehnke, U.-C., Remmler, T., Motschmann, H., Wurlitzer, S., Hauwede, J., and Fischer, T.M., *Partial air wetting on solvophobic surfaces in polar liquids.* Journal of colloid interface science, 1999. **211**(2): p. 243-251.
42. Tretheway, D., Stone, S., and Meinhart, C. *Effects of Absolute Pressure and Dissolved Gasses on Apparent Fluid Slip in Hydrophobic Microchannels*. in *APS Division of Fluid Dynamics Meeting Abstracts*. 2004.

43. Galea, T.-M. and Attard, P., *Molecular dynamics study of the effect of atomic roughness on the slip length at the fluid− solid boundary during shear flow.* Langmuir, 2004. **20**(8): p. 3477-3482.
44. Aktas, S., Kalyon, D.M., Marín-Santibáñez, B.M., and Pérez-González, J., *Shear viscosity and wall slip behavior of a viscoplastic hydrogel.* Journal of Rheology, 2014. **58**(2): p. 513-535.
45. Khosh Aghdam, S. and Ricco, P., *Laminar and turbulent flows over hydrophobic surfaces with shear-dependent slip length.* Physics of Fluids, 2016. **28**(3): p. 035109.
46. Watanabe, K., Udagawa, Y., and Udagawa, H., *Drag reduction of Newtonian fluid in a circular pipe with a highly water-repellent wall.* Journal of Fluid Mechanics, 1999. **381**: p. 225-238.
47. Zhu, Y. and Granick, S., *Limits of the hydrodynamic no-slip boundary condition.* Physical review letters, 2002. **88**(10): p. 106102.
48. Lauga, E. and Stone, H.A., *Effective slip in pressure-driven Stokes flow.* Journal of Fluid Mechanics, 2003. **489**: p. 55-77.
49. Lauga, E., Brenner, M.P., and Stone, H.A.J.a.p.c.-m., *Microfluidics: the no-slip boundary condition.* 2005.
50. Zhu, Y. and Granick, S., *Rate-dependent slip of Newtonian liquid at smooth surfaces.* Physical review letters, 2001. **87**(9): p. 096105.
51. Meeker, S.P., Bonnecaze, R.T., and Cloitre, M., *Slip and flow in pastes of soft particles: Direct observation and rheology.* J. Rheol., 2004. **48**: p. 1295–1320.
52. Kalyon, D.M., *Apparent slip and viscoplasticity of concentrated suspensions.* Journal of Rheology, 2005. **49**(3): p. 621-640.
53. Goyon, J., Colin, A., Ovarlez, G., Ajdari, A., and Bocquet, L., *Spatial cooperativity in soft glassy flows.* Nature, 2008. **454**(7200): p. 84-87.
54. Li, L., Su, Y., Wang, H., Sheng, G., and Wang, W., *A new slip length model for enhanced water flow coupling molecular interaction, pore dimension, wall roughness and temperature.* Adv. Polym. Technol., 2019. **1**.
55. Ortega-Avila, J.F., Perez-Gonzalez, J., Marın-Santiba˜nez, B.M., Rodrıguez-Gonzalez, F., Aktas, S., Malik, M., and Kalyon, D.M., *Axial annular flow of a viscoplastic microgel with wall slip.* J. Rheol., 2016. **60**(3): p. 503-515.
56. Yilmazer, U. and Kalyon, D.M., *Slip effects in capillary and parallel disk torsional flows of highly filled suspensions.* Journal of Rheology, 1989. **33**(8): p. 1197-1212.
57. Haase, A.S., Wood, J.A., Sprakel, L.M., and Lammertink, R.G., *Inelastic non-Newtonian flow over heterogeneously slippery surfaces.* Physical Review E, 2017. **95**(2): p. 023105.
58. Miao, Q., *Numerical study on the effect of wax deposition on the restart process of a waxy crude oil pipeline.* Advances in Mechanical Engineering, 2012. **4**: p. 973652.
59. Hoffmann, R. and Amundsen, L., *Single-phase wax deposition experiments.* Energy & Fuels, 2010. **24**(2): p. 1069-1080.
60. Bhat, N.V. and Mehrotra, A.K., *Modeling the effect of shear stress on the composition and growth of the deposit layer from "waxy" mixtures under laminar flow in a pipeline.* Energy fuels, 2008. **22**(5): p. 3237-3248.
61. de Souza Mendes, P.R., de Abreu Soares, F.S.-M., Ziglio, C.M., and Gonçalves, M., *Startup flow of gelled crudes in pipelines.* Journal of non-newtonian fluid mechanics, 2012. **179**: p. 23-31.
62. Chang, C., Nguyen, Q.D., and Rønningsen, H.P., *Isothermal start-up of pipeline transporting waxy crude oil.* Journal of non-newtonian fluid mechanics, 1999. **87**(2-3): p. 127-154.
63. Fakroun, A. and Benkreira, H., *Rheology of waxy crude oils in relation to restart of gelled pipelines.* Chemical Engineering Science, 2020. **211**: p. 115212.
64. Coussot, P., Nguyen, Q.D., Huynh, H.T., and Bonn, D., *Avalanche behavior in yield stress fluids.* Physical Review Letter, 2002. **88**(17): p. 175501.

65. Oishi, C.M., Martins, F.P., and Thompson, R.L., *The 'avalanche effect' of an elasto-viscoplastic thixotropic material on an inclined plane.* Non-Newtonian Fluid Mech, 2017. **247**: p. 165–177.
66. Ovarlez, G. and Coussot, P., *Physical age of soft-jammed systems.* Physical Review E, 2007. **76**(1): p. 011406.
67. Chambon, F. and Winter, H.H., *Stopping of crosslinking reaction in a PDMS polymer at the gel point.* Polymer Bulletin, 1985. **13**(6): p. 499-503.
68. Gunasekaran, S. and Ak, M.M., *Dynamic oscillatory shear testing of foods—selected applications.* Trends in Food Science Technology, 2000. **11**(3): p. 115-127.
69. Coussot, P., Tabuteau, H., Chateau, X., Tocquer, L., and Ovarlez, G., *Aging and solid or liquid behavior in pastes.* Journal of Rheology, 2006. **50**(6): p. 975-994.
70. Ovarlez, G. and Chateau, X., *Influence of shear stress applied during flow stoppage and rest period on the mechanical properties of thixotropic suspensions.* Physical Review E, 2008. **77**(6): p. 061403.
71. Coussot, P., Nguyen, Q.D., Huynh, H., and Bonn, D., *Viscosity bifurcation in thixotropic, yielding fluids.* Journal of rheology, 2002. **46**(3): p. 573-589.
72. Malkin, A.Y., *Flow instability in polymer solutions and melts.* Polymer Science Series C, 2006. **48**(1): p. 21-37.
73. Ragouilliaux, A., Herzhaft, B., Bertrand, F., and Coussot, P., *Flow instability and shear localization in a drilling mud.* Rheologica acta, 2006. **46**(2): p. 261-271.
74. Hays, C., Kim, C., and Johnson, W.L., *Microstructure controlled shear band pattern formation and enhanced plasticity of bulk metallic glasses containing in situ formed ductile phase dendrite dispersions.* Physical Review Letters, 2000. **84**(13): p. 2901.
75. Joshi, Y.M., *Model for cage formation in colloidal suspension of laponite.* Journal of Chemical Physics, 2007. **127**: p. 081102-5.
76. Ruzicka, B. and Zaccarelli, E., *A fresh look at the Laponite phase diagram.* Soft Matter, 2011. **7**(4): p. 1268-1286.
77. Delhorme, M., Jönsson, B., and Labbez, C., *Monte Carlo simulations of a clay inspired model suspension: the role of rim charge.* Soft Matter, 2012. **8**(37): p. 9691-9704.
78. Pignon, F., Magnin, A., Piau, J.-M., Cabane, B., Lindner, P., and Diat, O., *Yield stress thixotropic clay suspension: Investigations of structure by light, neutron, and x-ray scattering.* Physical Review E, 1997. **56**(3): p. 3281.
79. Tanaka, H., Jabbari-Farouji, S., Meunier, J., and Bonn, D., *Kinetics of ergodic-to-nonergodic transitions in charged colloidal suspensions: Aging and gelation.* Physical Review E, 2005. **71**(2): p. 021402.
80. Ruzicka, B., Zulian, L., Angelini, R., Sztucki, M., Moussaid, A., and Ruocco, G., *Arrested state of clay-water suspensions: Gel or glass?* Physical Review E, 2008. **77**(2): p. 020402.
81. Cocard, S., Tassin, J.F., and Nicolai, T., *Dynamical mechanical properties of gelling colloidal disks.* Journal of Rheology, 2000. **44**(3): p. 585-594.
82. Instruments, B.a., *LAPONITE – Performance Additives*. 2014, BYK Additives & Instruments.
83. Tanaka, H., Meunier, J., and Bonn, D., *Nonergodic states of charged colloidal suspensions: Repulsive and attractive glasses and gels.* Physical Review E, 2004. **69**: p. 031404.
84. Joshi, Y.M., Reddy, G.R.K., Kulkarni, A.L., Kumar, N., and Chhabra, R.P., *Rheological behaviour of aqueous dispersions of Laponite: new insights into the ageing phenomena.* Proceedings of the Royal Society A, 2008. **464**: p. 469–489.
85. Mourchid, A. and Levitz, P., *Long-term gelation of Laponite aqueous dispersions.* Physical Review E, 1998. **57**(5): p. R4887–R4890.
86. Mongondry, P., Nicolai, T., and Tassin, J.F., *Influence of pyrophosphate or polyethylene oxide on the aggregation and gelation of aqueous Laponite dispersions.* Journal of Colloid and Interface Science, 2004. **275**(1): p. 191–196.

87. Rich, J.P., McKinley, G.H., and Doyle, P.S., *Size dependence of microprobe dynamics during gelation of a discotic colloidal clay.* Journal of Rheology, 2011. **55**(2): p. 273-299.
88. Felix K. Oppong, P. Coussot, and Bruyn, J.R.d., *Gelation on the microscopic scale.* Physical Review E, 2008. **78**: p. 021405.
89. Shahin, A. and Joshi, Y.M., *Physicochemical effects in aging aqueous Laponite suspensions.* Langmuir, 2012. **28**(44): p. 15674-15686.
90. Lin, Y., Zhu, H., Wang, W., Chen, J., Phan-Thien, N., and Pan, D., *Rheological behavior for laponite and bentonite suspensions in shear flow.* AIP Advances, 2019. **9**(12): p. 125233.
91. Siqueira, I.R., Pasquali, M., and de Souza Mendes, P.R., *Couette flows of a thixotropic yield stress material: performance of a novel fluidity-based constitutive model.* Journal of Rheology, 2020. **64**(4): p. 889-898.
92. Escudier, M.P. and Presti, F., *Pipe flow of a thixotropic liquid.* Journal of Non-Newtonian Fluid Mechanics, 1996. **62**(2-3): p. 291-306.
93. Biswas, R., Saha, D., and Bandyopadhyay, R., *Quantifying the destructuring of a thixotropic colloidal suspension using falling ball viscometry.* Physics of Fluids, 2021. **33**(1): p. 013103.
94. Crocker, J.C. and E.R., W. *Particle tracking using IDL*. 2006; Available from: http://www.physics.emory.edu/faculty/weeks//idl.
95. Nguyen, N.T., *Micromixers: fundamentals, design and fabrication*. 2011: Elsevier.
96. Poumaere, A., Moyers-Gonz alez, M., Castelain, C., and Burghelea, T., *Unsteady laminar flows of a carbopol gel in the presence of wall slip.* J. Non-Newtonian Fluid Mechanics, 2014. **205**: p. 28.
97. Cheng, J.T. and Giordano, N., *Fluid flow through nanometer-scale channels* Phys. Rev. E, 2002. **65**: p. 031206.
98. Pek-Ing, A. and Yee-Kwong, L., *Surface chemistry and rheology of Laponite dispersions—Zeta potential, yield stress, ageing, fractal dimension and pyrophosphate.* Applied Clay Science, 2015. **107**: p. 36-45.
99. Ranganathan, V.T. and Bandyopadhyay, R., *Effects of aging on the yielding behaviour of acid and salt induced Laponite gels.* Colloids Surfaces A: Physicochemical Engineering Aspects, 2017. **522**: p. 304-309.
100. Suman, K. and Joshi, Y.M., *Microstructure and soft glassy dynamics of an aqueous laponite dispersion.* Langmuir, 2018. **34**(44): p. 13079-13103.
101. Joshi, Y.M. and Petekidis, G., *Yield stress fluids and ageing.* Rheologica Acta, 2018. **57**(6): p. 521-549.

Appendix A

Experimental System Design and Operational Issues

The experimental set-up went through several iterations during the initial phase of this work, to address critical shortcomings in the protocol. The learnings from these changes in experimental design are summarized in this Appendix. Over here we discuss the several experimental design and operating features which were unsuccessful, but nevertheless pointed towards the final optimized experimental system and operations described in Chapter 3.

All the experiments described in the following sections are performed with Laponite suspension in water for concentrations below 3wt%. The sample was prepared using experimental set-up as described below for concentrations less than 3wt%.

A.1. Experimental protocol

As suspension shows time dependent aging property and shear sensitive mechanical property, the results of continuous flow experiments can vary with experimental protocol. There are 3 possible experimental protocols those can be employed for the pipe flow study of LAPONITE® suspension:

1) Initiate flow with desired concentration of LAPONITE® in the vessel and pipe
   Different aging behaviors are expected inside the tube: One due to the time dependent behaviour for the quiescent suspension and other due to the effect of flow. At high concentrations, experimental results may vary with each run and also may vary how the suspension was filled in the tube

2) Start with desired LAPONITE® suspension in the tank and pre-fill pipe with water
   It required a long time to reach the steady state concentration in pipe wherein LAPONITE® suspension replaces the water eventually.

3) Start with a lower concentration in vessel and slowly increase to the desired value
   Experiments were performed with this protocol. The related results and experimental difficulties are described below.

Initially two separate volumes of LAPONITE® dispersion (25 ml to fill the pipe completely and 20 ml in the mixing tank) are made lower than the desired LAPONITE® concentration by vigorous mixing of dried power in NaCl solution in the tank for 30 min at a high speed of 5000 rpm. Under vigorous stirring, the suspension becomes transparent. Following this, NaCl solution and LAPONITE® powder, which makes desired concentration of suspension, are added continuously in one of the tank containing 20 ml premixed suspension at a pre-defined rate. Flows of both streams are set by the syringe pump. Schematic of the experimental setup is shown below. At the same time, suspension is pumped from the tank to a pipe of 1 cm diameter and 2 ft length keeping input flow rate constant. The pipe is pre-filled with a separately pre-mixed 25 ml suspension. The Laponite concentration, then, rises slowly in the tank as well as in the pipe to a desire concentration without altering salt concentration (C_s = 3 mM). Then pressure drop across the pipe is recorded over time. The flow rate is monitored at the outlet during the experimental run to ensure constant flow condition. Here in experiments, we have used a glass tube having both ends tapered to reduce entry and exit losses, if any.

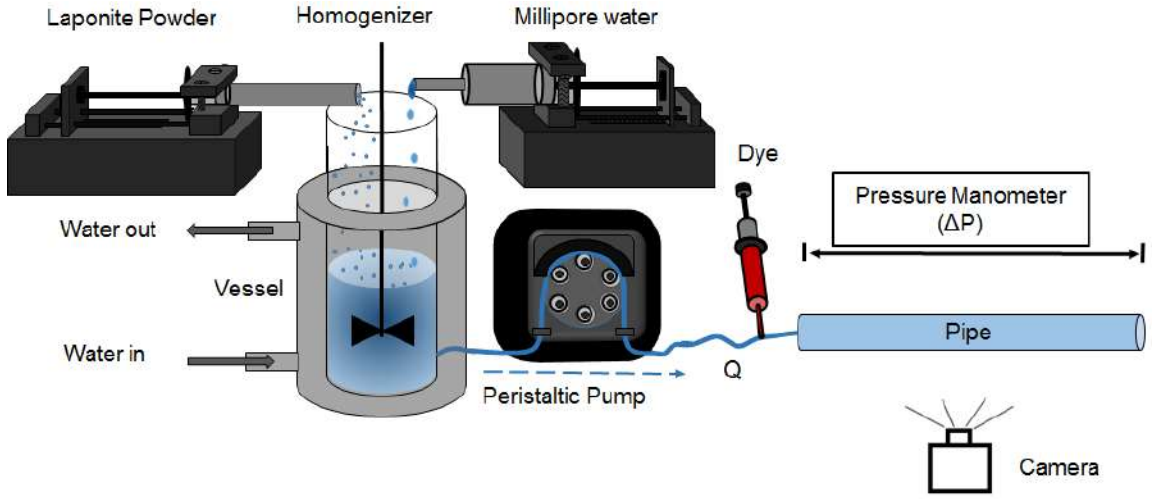

Figure A.1 Schematic of continuous flow process for LAPONITE® suspension preparation.

A.2 Experimental results

Once continuous flow is started, concentration in the tank is estimated based on equation below as given in table A-1, derived from steady state mass balance assuming a well mixed tank.

$$C_{lap}(\mathrm{t}) = C_{in} + (C_0 - C_{in}) \exp\left(-\frac{t}{\tau}\right) \tag{A.1}$$

Table A-1 Concentration inside the tank based on given input parameters is estimated using expression in equation (A.1).

Desired concentration (C_{lap})	C_0	C_{in}	$\frac{C_{lap}(t = 60\mathrm{min})}{C_{lap}} * 100$
2.9 wt%	2.7 wt%	2.9 wt%	98 %
2.8 wt%	2.6 wt%	2.8 wt%	98 %
2.4 wt%	2.2 wt%	2.4 wt%	98 %

where, C_{in} and C_0 are the concentrations of LAPONITE® in inlet stream and initial concentration inside the tank. $C_{lap}(t)$ is time dependent LAPONITE® concentration inside the tank. τ = 50 mins is the residence time in the pipe (obtained as the ratio of the pipe volume to the volumetric flow rate specified by the pump). Within 1 hour, concentration nearly reaches to 98% of desired LAPONITE® concentration based on eq. A.1. The time dependent data in this 1 hour that is taken to achieve steady state concentration is not considered. Then pressure drop across the pipe (of diameter 1 cm and 30 cm length) is recorded as a function of time for the set flow rate (0.4 ml/min). Variation in pressure drop (ΔP) and volumetric flow rate (Q) during experimental run is plotted in fig. A.1 for 2.9 wt% LAPONITE® and 3 mM salt concentration. At t = 0, pressure drop in pipe is nearly 5 kPa and further rises with time. Then there is a sudden increase in pressure drop nearly after 70 min of continuous flow of suspension inside the pipe. Later pressure drop shows large variations. Pressure drop sometime keeps on increasing beyond the pressure manometer limit (see repeated data e, c and d in fig. A.2I). While in some of the repeated test a, b and f, pressure drop decreases for a while after initial peak, then again there is a sudden increase in pressure drop. However, the outlet flow rate was approximately constant over experimental time scale even during sudden increase in pressure drop as shown in fig. A.2II). Here, volumetric flow rate is calculated by collecting samples volume at the outlet of pipe for 4 to 5 minutes. Further we vary LAPONITE® concentration from 2.4 to 2.8 wt%. It is worth noting that pressure drop response is same for both LAPONITE® concentrations (refer fig. A.3) as observed for 2.9 wt%.

Initial pressure jump after 70 minutes of flow is evident in all cases. We discuss the reason for this pressure jump in the following section.

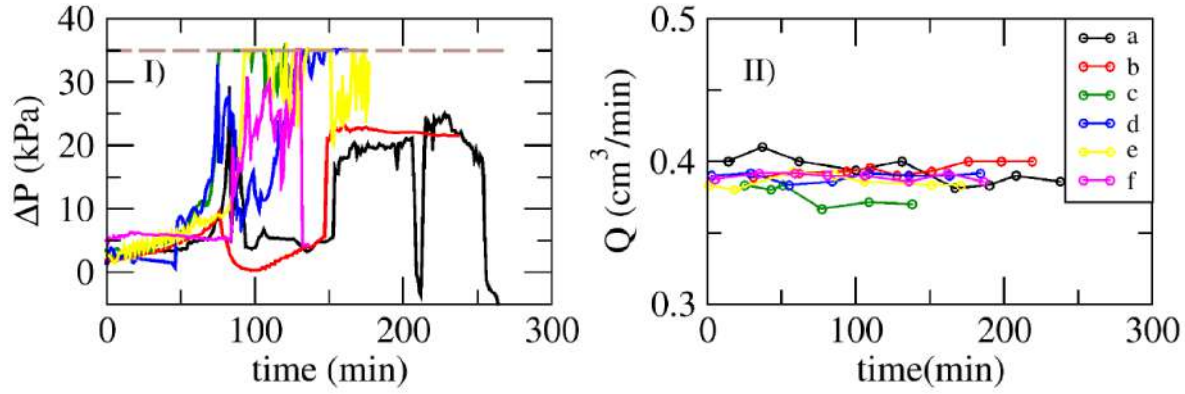

Figure A.2 I) Time dependent pressure drop response and II) respecctive volumetric flowrate are measured for flowing LAPONITE® suspension at set rate 0.4 cm^3/min. Experimental repeatations are shown by different colors. Dashed horiontal line represents maximum pressure sensing limit of manometer. The curves of different color (a-f) represent repeated experimental data.

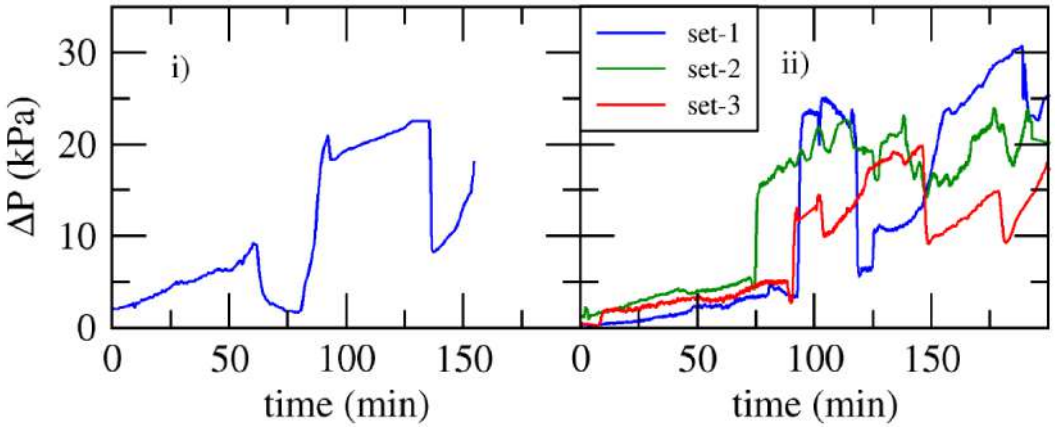

Figure A.3 Pressure (ΔP) exerted by flowing LAPONITE® suspension of concentration i) C_{lap} = 2.4 wt% and ii) C_{lap} = 2.8 wt% through a tube (of diameter 1 cm and 30 cm length) is measured as a funtion of experimental time maintaining C_s = 3 mM salt in suspension.

It is assumed here that suspension viscosity at the inlet of pipe does not change over a period of time. At t = 0, the well mixed suspension of 98% of desired concentration is pumped into

the pipe. A minimum of 60 minutes is required to fill the entire tube with LAPONITE® suspension. At the beginning, freshly prepared clay dispersion inside the pipe is a liquid sol. The pressure drop to pump this through the pipe is, thereby, quite low. Due to low shear rate and large residence time (60 min) inside the pipe, the suspension is expected to age with time. By the time it reaches the tube exit, suspension becomes highly viscous. The first pressure peak between about 60 – 100 min, occurs when this highly viscous suspension flows out through the tapered end. The pressure jump is quite reproducible in all cases (see fig. A.2 and fig. A.3). This is an inherent outcome of the implemented protocol. We believe that the suspension pre-filled inside the pipe and that pumped into the pipe age differently. As a result, microstructure forms inside the pipe and that dislocates (at around 70 - 90 minutes of experimental run) when the suspension becomes viscous enough. As dislocation process and initial structure formation process are random, the first pressure peak position and its strength (i.e. ΔP values) vary. Then, we have further modified the experimental protocol by filling an experimental tube with water initially (in place of LAPONITE® concentration) and started with desired LAPONITE® concentration.

A.3 Effect of tapering tube

At the beginning, the experimental pipe used for the study has tapering ends. We have investigated pipe flow behavior with and without tapering pipe end. Given the suspension time dependent behavior, we expect that the tapered section at the end of pipe would have additional effect which is discussed below.

An experimental assembly comprising continuous stirred tank is used (refer fig. A.1) for LAPONITE® suspension preparation employing the procedure as follows. LAPONITE® powder is dried at 120^{o}C for 4 hours to remove moisture. Then dry powder is maintained at 50^{o}C and used in experiment as required. Initially, LAPONITE® suspension of desired concentration is prepared in the tank by vigorous mixing at 4000 rpm for 30 minutes. Then dry powder at a pre-defined mass rate and water/ aqueous salt solution also at pre-defined mass rate are added continuously into the tank containing premixed suspension of LAPONITE®. During experimental run, suspension inside the tank is kept under stirring at constant speed. Simultaneously, the mixed suspension is pumped to an experimental pipe which is initially filled with water. The pumped suspension slowly replaces the water volume over time. The pressure measurements were started once LAPONITE®

suspension fills the entire pipe volume. A digital camera (Logitech HD 1080p) is installed near the pipe to visualize the bulk flow along pipe length. For visualization purpose, a pulse of red and blue color food dye is injected alternately for a short duration at the pipe inlet. A sequence of images of flowing suspension is captured at rate of 1/5 frame/s throughout experimental run. The material is collected at the tube outlet to verify the constant flow condition during run.

A.3.1 Effect of tube exits: Tapered ends

Initial experiments were performed in a tube (D = 1 cm and L = 30 cm) having both ends tapered. Tube entrance has a uniformly diverging taper section (0.1 cm to 1 cm) of length 2 cm and a uniformly converging taper section (1 cm to 0.1 cm) of length 2 cm at the tube exit. Pressure drop across pipe length is recorded after 70 minutes of continuous pumping at pre-defined rate of 0.4 ml/min so that LAPONITE® suspension fills the entire pipe volume. It is observed that for 1.4 wt% LAPONITE® concentration, the pressure drop is negligible and remains constant during the entire run (see fig. A.4i). At lower concentration of suspension, about 1.4wt%, aging is expected to be negligible. Consequently, there is no significant structure formation during experimental run. Hence, pressure drop required to pump the suspension through the tube cannot be resolved with the digital manometer used. Further we have varied LAPONITE® concentrations (1.6, 1.8, 2.2 and 2.4 wt%) and time dependent responses for all the concentrations are displayed in fig. A.4. At t = 0 min, pressure drop is approximately 1 kPa for LAPONITE® concentrations from 1.6 to 2.2 wt%. This suggests same suspension state/structure inside the tube at the beginning. Then ΔP rises in time for a certain period indicative of formation of viscous material inside the pipe and decrease back to 1 kPa suggesting release of viscous material out of the tube. Again, the pressure rises followed by multiple decreases while the suspension flows through the pipe. Mostly, pressure growth is gradual for lower concentration while it rises more rapidly at higher concentration. Rather the decreasing ΔP response is sudden. For a given concentration, experiment is repeated 2-3 times. The time dependent pressure response is not systematic and is quantitatively irreproducible (see repeated data set represented by different colors in fig. A.4). But the qualitative behavior is qualitatively same. The amplitude and frequency of pressure fluctuations increases with LAPONITE® concentration from 1.6 wt% to 2.2 wt% (see fig. A.4ii-iv). For increased LAPONITE® concentrations, pressure drop exhibits more frequent fluctuations and the minimum

pressure value increases to 5 kPa while average pressure drop increases. The data shown in fig. A.4v for C_{lap} = 2.4 wt% is qualitatively different than the others.

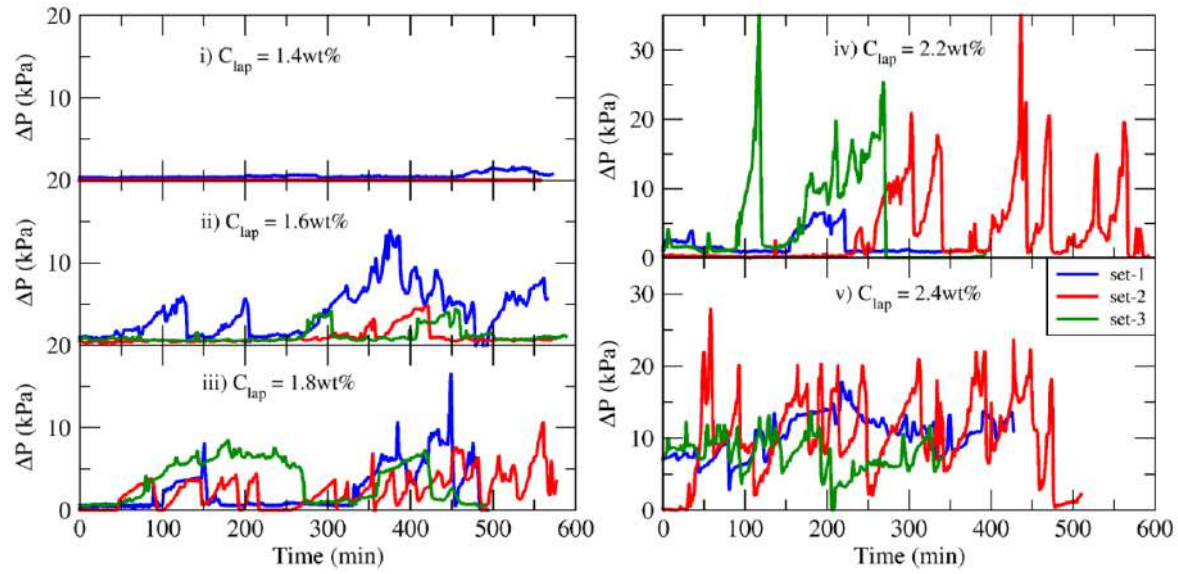

Figure A.4 Pressure drop across the tube (D = 1 cm, L = 30 cm) having tapered ends with respect to experimental time is measured for different LAPONITE® concentration: i) C_{lap} = 1.4 wt%, ii) C_{lap} = 1.6 wt%, iii) C_{lap} = 1.8 wt%, iv) C_{lap} = 2.2 wt% and v) C_{lap} = 2.4 wt%. All experiements were performed at fixed salt concentration (C_s = 3 mM) and flowrate (Q = 0.4 ml/min). Different color line represents repeated experimental runs.

To correlate flow nature with pressure response, we have visualized the entire pipe flow during pressure measurement. Red and blue color food dye were used for visualization purpose. When dyed suspension flows through a pipe, color will help to differentiate a blocked and flow region. Aqueous solution of dye is prepared by dissolving very small quantity of dye powder. Each dye solution is added alternatively in very small quantity at the inlet of pipe for few minutes. There is no dye addition between two pulses of different color dye. The sequence of RGB images were taken at rate of 12 frames/minute using a Web camera.

When red dye is injected in a line, the dye flows through the pipe center up to few centimeters distance from the entrance showing channel flow embedded by solid like gel at t = 02:05 min:sec (see red color region-II of fig. A.5iii). Further the red dye spreads across the cross-section suggesting dislocation of entrance blocked region (see region-II in fig. A.5iii and iv). Same

flow nature is also clearly seen from overall flow sequence of images where red colored region-I moves horizontally (see fig. A.5ii and iv). Some extent of dye diffusion is expected during flow which is in the case of Region-II observed where upstream red color line disappeared over time (from fig. A.5iii-v). Here, exact phenomenon for pressure response cannot be correlated with the flow without knowing the inlet-outlet flow conditions. After 37 minutes, blue dye is added in flowing stream. Region-III, which comprises a faint blue color area, shows channel flow surrounded by transparent static gel, while upstream section flows like a plug. Then blue color addition continues for another 13 minutes. Within this period, the color fills the space behind the Region-II. Combined channel flow at the pipe entrance and upstream plug flow continues further and is visible till 63 minutes (see blue and red colored region movement in fig. A.5vi and vii). During this period, the red colored Region-II (which initiated at 02:05 min:sec) moves towards pipe exit. As soon as this red colored plug pushes through the tapered pipe end (see fig. A.5viii), the pressure drop suddenly increases (see fig. A.5i). At the same instant, the entrance blocked region (transparent area which encloses channel flow exposed by blue dye addition refer fig. A.5vi and vii) dislocates. However, it is worth reporting that added blue solution becomes highly viscous and sticks to the wall allowing the flow to occur through the center channel as seen through progressive images (see fig. A.5vii-ix)

(i)

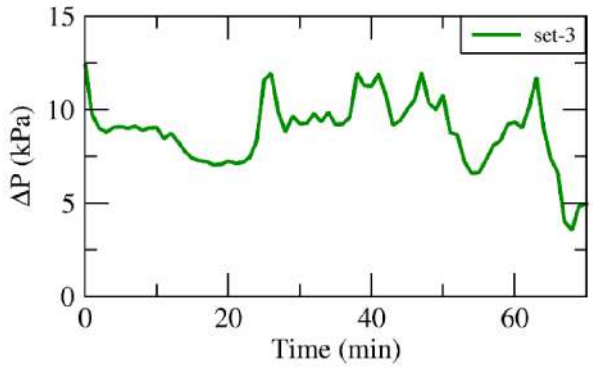

(ii) t = 00:00 min:sec

(iii) t = 02:05 min:sec; Red color just started adding for 18 minutes in the flowing line to visualize flow path inside the pipe.

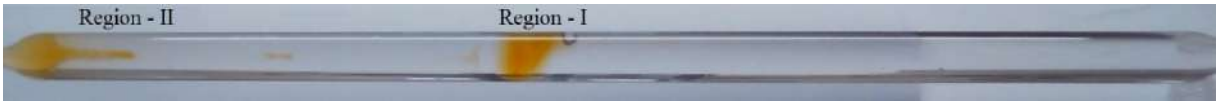

(iv) t = 18:20 min:sec; Stopped red color adding in the flowing line

(v) t = 37:00 min:sec; No color adding in the system

(vi) t = 39:10 min:sec; Blue color added in the line

(vii) t = 50:50 min:sec; Stopped blue color adding after 13 minutes

(viii) t = 57:55 min:sec; no dye in flowing stream

(ix) t = 63:00 min:sec; Started red color adding in the system

Figure A.5 Time dependent (i) pressure evolution and (ii) - (ix) simultanuous flow visualization with a dye inside the pipe (D = 1cm, l = 30cm) during suspension flow (C_{lap} = 2.4wt% & C_s =

3mM). The images are taken at different times when no color added in the line ((ii), (v) and (viii)), when red food dye is injected in a line ((iii) – (iv) and (ix)) and when blue color added in the line ((vi) – (vii)). Suspension flows from left to right in a pipe. Different color inside the pipe indicates different material aging times.

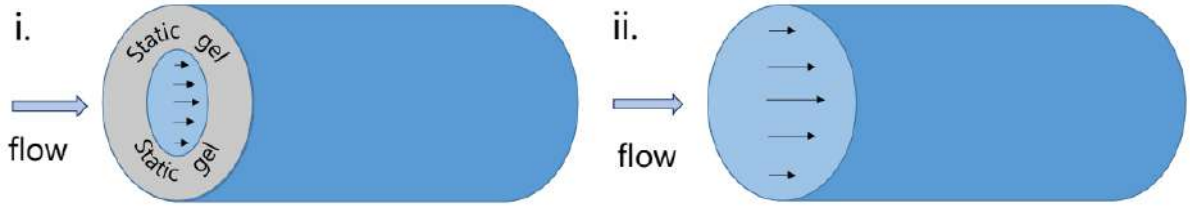

Figure A.6 Schematic representation of different types of flow occurs during experimental run. i. Flow through a channel ($A_c < A_p$) and ii. Flow through a complete pipe area.

It is observed that there are two flow regimes which exist during the flow. One is flow through an entire pipe cross-section of pipe and other is flow through a channel. The representation of both flow is shown in fig. A.6. Knowing suspension behavior, highly viscous like state of suspension is expected towards the pipe exit as it has aged for long time, when suspension flows through an entire pipe cross-section for sufficiently longer time than liquid-solid transition time. At this state, it flows as a solid plug observed during flow. It is reported for aging fluids that there exists a solid like viscous material at the center of pipe and liquid like behavior at pipe wall. But our experiments show completely opposite phenomenon, i.e channel flow at the center of the pipe as shown in fig. A.6i. However, channel formation is random and can form any radial position. It is interesting how this channel formation occurs. But, due to inadequate imaging facility we could not explore further. From flow visualization, two mechanism can be attributed for the observed pressure jumps: 1) squeezing of highly viscous gel like solid material through a tapered end; 2) dislocation of static gel which blocked the flowing area near the wall. Both phenomena occur during flow. It is very difficult to correlate both these mechanisms across pressure drop measurements and flow visualization. We believe that the dislocation of the occluded area results in an instant pressure spike. Squeezing a solid plug through the smaller outlet will lead to higher pressure drop till viscous material flows completely out of the tube.

A.3.2 Tube with tapered inlet

To separate the squeezing effect and dislocation effect, suspension is flown through a tube without a tapered outlet which maintaining the tapered inlet (as shown in image fig. A.8b and c). Using this tube, no squeezing effects are expected. In fig. A.7, changes in pressure drop across the tube is compared with data measured for a tube having tapered end during suspension (C_{lap} = 2.4wt%, C_s = 3mM) flow at 0.4ml/min. There are no pressure fluctuations for the flow occurring through an exit without tapered section. By comparing pressure data for both cases, flow through a pipe with and without tapered end, it suggests there is major contribution of squeezing phenomenon due to tapered end. However, the gel dislocation effects still persists in the system that can influence pressure drop measurements.

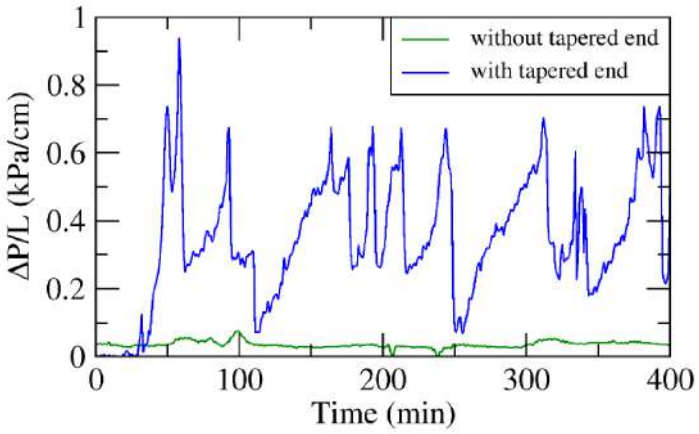

Figure A.7 Time dependent variation in pressure drop per unit length ($\Delta P/L$) for a same pipe diameter (D = 0.72 cm) and same suspension concentration with and without tapered pipe outlet.

To confirm the blocked dislocation in system, red and blue color food dyes are added during flow in very small quantity at the pipe inlet. It takes few seconds for the dye to enter the pipe. Within that short time period, the color mixes almost uniformly in the flowing stream, rather than flowing along a streamline without mixing. The visualization shows a flow through a narrow passage surrounded by relatively static highly viscous LAPONITE® fluid. Displayed images in Figure A.8b, blue color region show the flowing suspension and transparent blocked region. There is an instant spike in pressure drop only whenever the blocked area dislodges (see fig. A.8a). Otherwise, the pressure drop stays constant. Plug dislocation effect is an instantaneous event and

it is clearly visible from fig. A.8c. Red color is injected in line followed by blue color. The red color dye which replaced the channel blue color, intermediately spreads across the pipe cross-section at the pipe entrance, indicating moving blocked region which can be also seen from trapped air bubbles movements. This describes block dislocation phenomena. However, the pressure response is not the same whenever food dye is absent. We further assume that there might be some physical or chemical interactions between the food dye and LAPONITE® suspension. The study of this origin significantly diverts from our primary objective of the study. Hence, we consider only the weak pressure signal during actual suspension flow. To amplify the dislocation effects, we have tried varying the suspension concentration. Higher concentration means higher strength of static plug which will reflect in higher pressure drop. But suspension preparation at higher concentration is much more difficult task due to rapid aging. There are other issues related to mixing and powder sticking while preparation. These have been discussed in detail in Chapter 3.

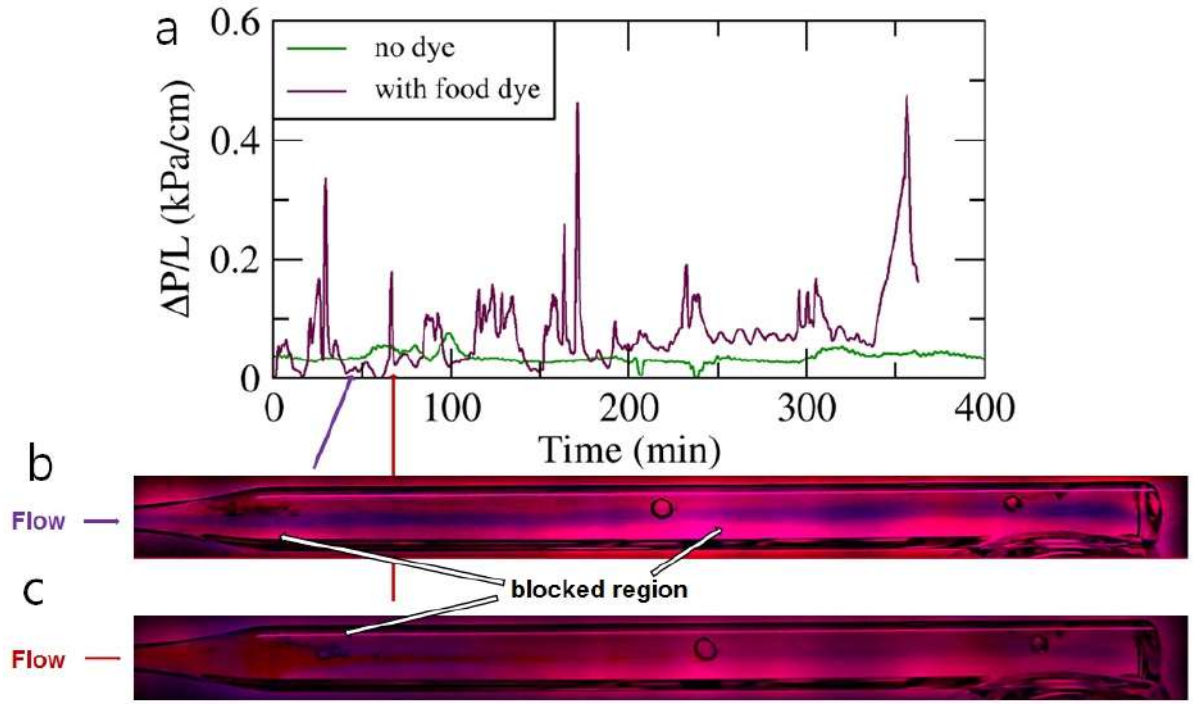

Figure A.8 Comparison between pressure drop response of with and without food dye addition in flowing LAPONITE® suspension (C_{lap} = 2.4wt%, C_s = 3mM) throught a pipe (D = 0.72cm and L = 10cm) having tapered inlet. Images during adition of b. blue dye color showing channel flow and c. red color showing in-stiu block dislocation phenomenon are captured.

ABSTRACT

Name of the Student: Prophesar M. Kamdi
Registration No. : 20EE14A2607
Faculty of Study: Engineering Sciences
Year of Submission: 2021
AcSIR academic centre/CSIR Lab: NCL - Pune
Name of the Supervisor(s): Dr. Ashish V. Orpe
Dr. Guruswamy Kumaraswamy

Title of the thesis: Study of pressure driven flow of Laponite suspension through a cylindrical tube

Several industrial applications handle materials which tend to cause clogging while flowing through conduits, orifices, channels etc. The blockage results in reduced cross sectional area available for flow. This can occur when either the individual constituent or entities have sizes comparable to the flow area or if they agglomerate over time leading to bigger entities which block the flow. The latter type of clogging is due to time dependent or thixotropic materials. Investigating the phenomena of flow and clogging caused due to time varying state of the material flowing through pipes forms the primary objective of this work.

For time dependent flow study, experiments were conducted by flowing a LAPONITE® suspension with salt addition in a pulse manner through a cylindrical tube having tapered inlet. The experimental study shows steady state pressure drop response exhibiting familiar Poiseuille dependence on pipe diameter, pipe length and salt concentration for thixotropic suspension. However, the pressure drop per unit length shows a monotonic decrease with increase in flow rate which is qualitatively opposite to Poiseuille pipe flow behavior. The above mentioned behaviours were recovered theoretically by assuming (i) the LAPONITE® suspension exhibiting Bingham fluid like rheology (ii) presence of yielding at the tube walls confirmed through flow visualization (iii) linear dependence of slip length on flow rate and (iv) suspension viscosity exhibiting power law dependence on salt concentration.

While it is acknowledged that the scaling relation (an empirical correlation among slip length, pipe diameter and flow rate) is purely based on a fit to the data, given that some of the assumed variations could not be ascertained from the literature, the reasonably good scaling behavior suggests that the adhoc assumptions are not without merit. Moreover, the scaling relation can be considered as a first step towards a comprehensive understanding of the flow of thixotropic materials through pipes and can act as a foundation for a more involved theoretical treatment in future.

Details Of Publications

List of publications emanating from thesis

1. ***Prophesar M. Kamdi,*** Ashish Orpe, Guruswamy Kumaraswamy, Slip behavior during pressure driven flow of Laponite suspension, Physics of Fluids, 33, 053102(2021) *DOI: https://doi.org/10.1063/5.0051044*